US005889807A

United States Patent [19]

Cunningham et al.

[11] Patent Number: 5,889,807

[45] Date of Patent: Mar. 30, 1999

[54] **HIGH POWER PHOTOLYTIC IODINE LASER**

[76] Inventors: **Philip R. Cunningham**, 5 Falcon Ct. W., Edgewood, N. Mex. 87015; **Robert A. Rathge**, 9105 Lagrina De Oro, NE., Albuquerque, N. Mex. 87111; **Leon A. Baros**, Star Rte. Box 50, Ribera, N. Mex. 87560; **LaVerne A. Schlie**, 7503 Lamplighter La., NE., Albuquerque, N. Mex. 87109; **Sallie S. Townsend**, 119 Coleman Rd., Manchester, Conn. 06040-3310; **John J. Hinchen**, 56 Jean Rd., Manchester, Conn. 06040

[21] Appl. No.: **948,753**

[22] Filed: **Oct. 10, 1997**

Related U.S. Application Data

[63] Continuation-in-part of Ser. No. 651,471, May 22, 1996, Pat. No. 5,802,093.

[51] **Int. Cl.**[6] **H01S 3/22**; H01S 3/223

[52] **U.S. Cl.** **372/55**; 372/58

[58] **Field of Search** 372/55, 58, 64, 372/70, 84

[56] **References Cited**

U.S. PATENT DOCUMENTS

5,425,044 6/1995 Schlie et al. 372/55

Primary Examiner—Rodney Bovernick
Assistant Examiner—Robert E. Wise
Attorney, Agent, or Firm—McCormick, Paulding & Huber

[57] **ABSTRACT**

A continuous wave photolytic iodine laser has a gain cell for receiving a continuous supply of gaseous fuel. The gain cell is connected to laser beam transfer optics, a laser resonator for shaping a laser beam, and a lamp. The lamp is driven by a microwave subsystem such that a laser gain medium is pumped through the gain cell. The continuous wave photolytic iodine laser of the present invention incorporates a closed loop fuel system for presenting gaseous fuel to the gain cell at a rate sufficient to sweep any lasing by-products out of the gain cell, thereby preventing quenching of the lasing process. The fuel system also includes a condenser for converting the gaseous fuel to a liquid after it has passed through the gain cell, a scrubber for removing the by-products of the lasing process from the fuel, and an evaporator for converting the recycled liquefied fuel back to a gas. The closed loop fuel system also includes a pump for pressurizing and transporting the liquefied fuel.

36 Claims, 20 Drawing Sheets

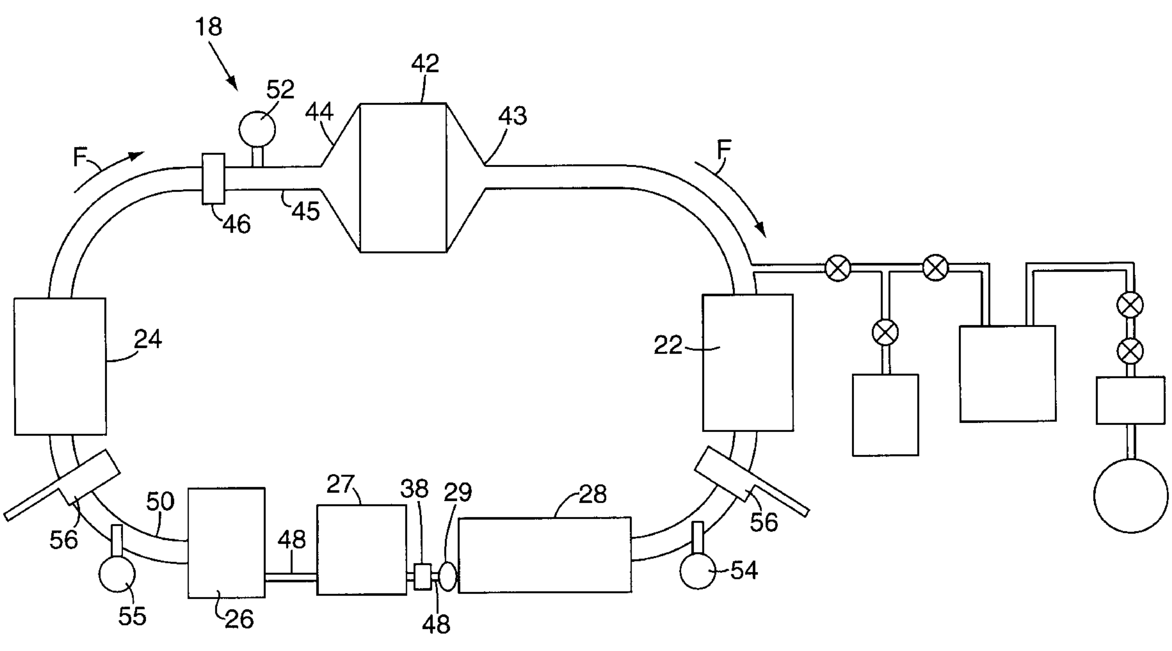

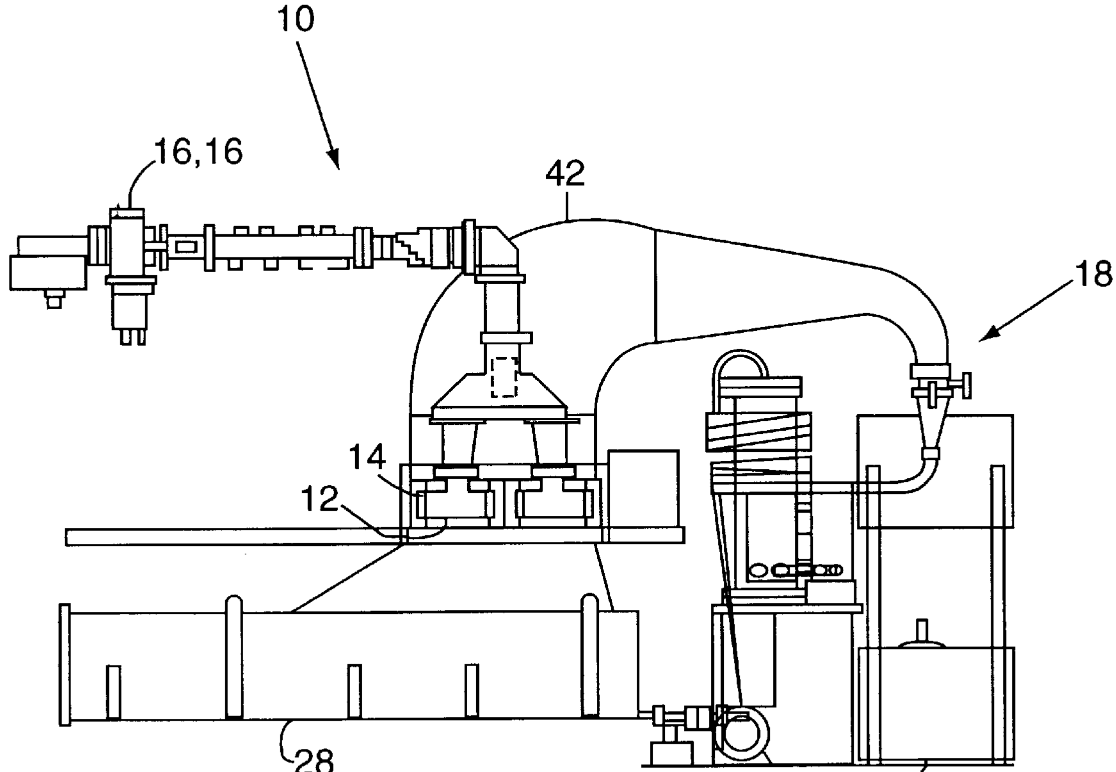

FIG. 1

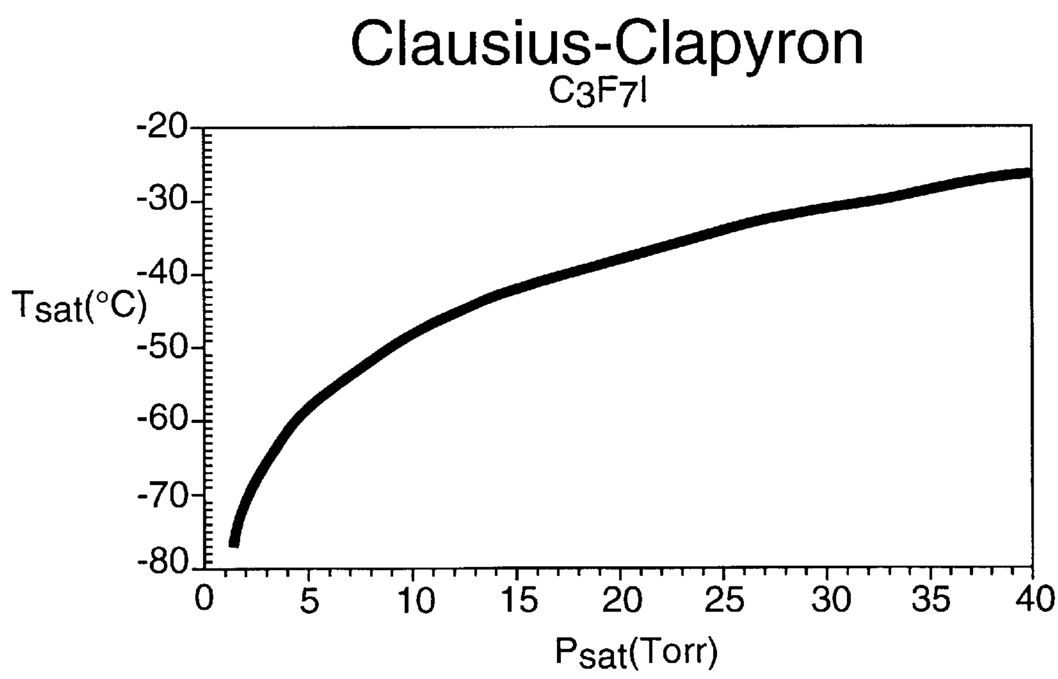

C3F7I vapor pressure curve

FIG. 4

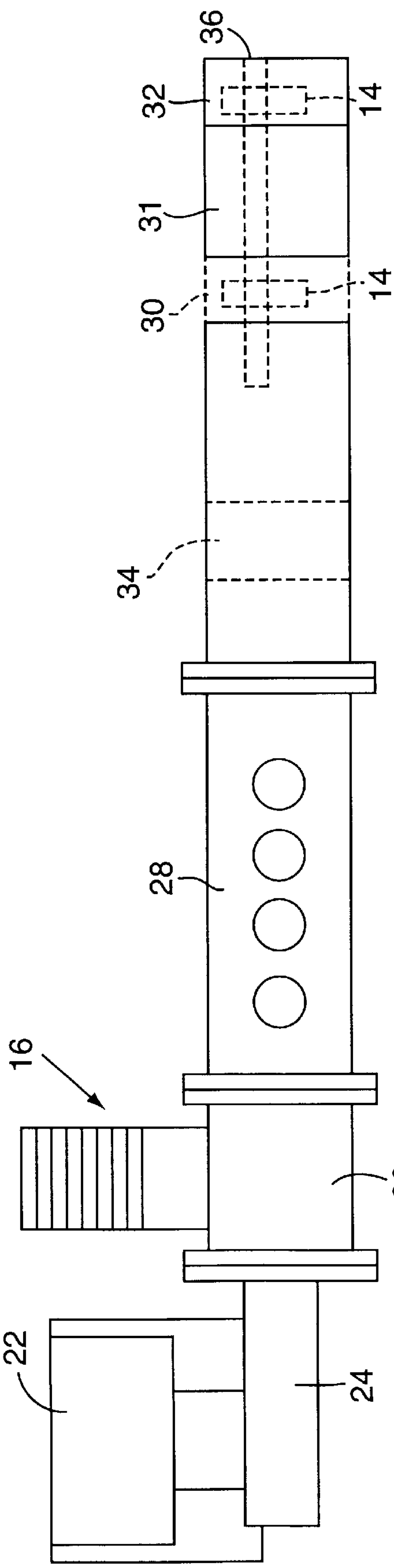

FIG. 2

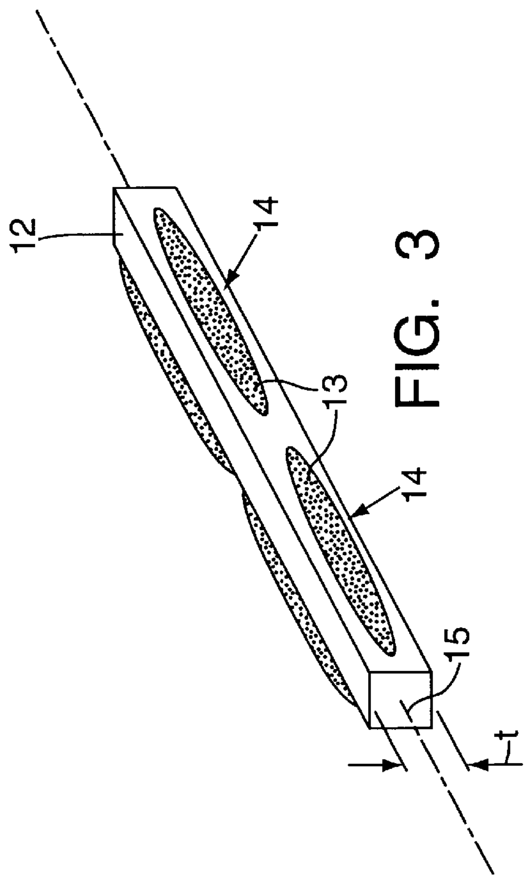

FIG. 3

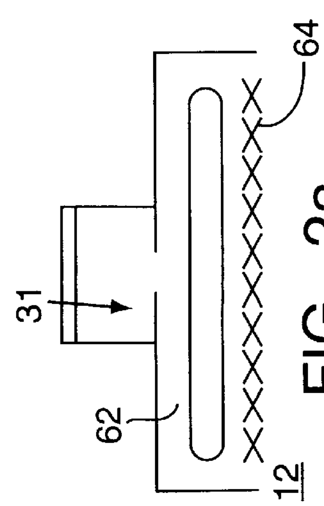

FIG. 2a

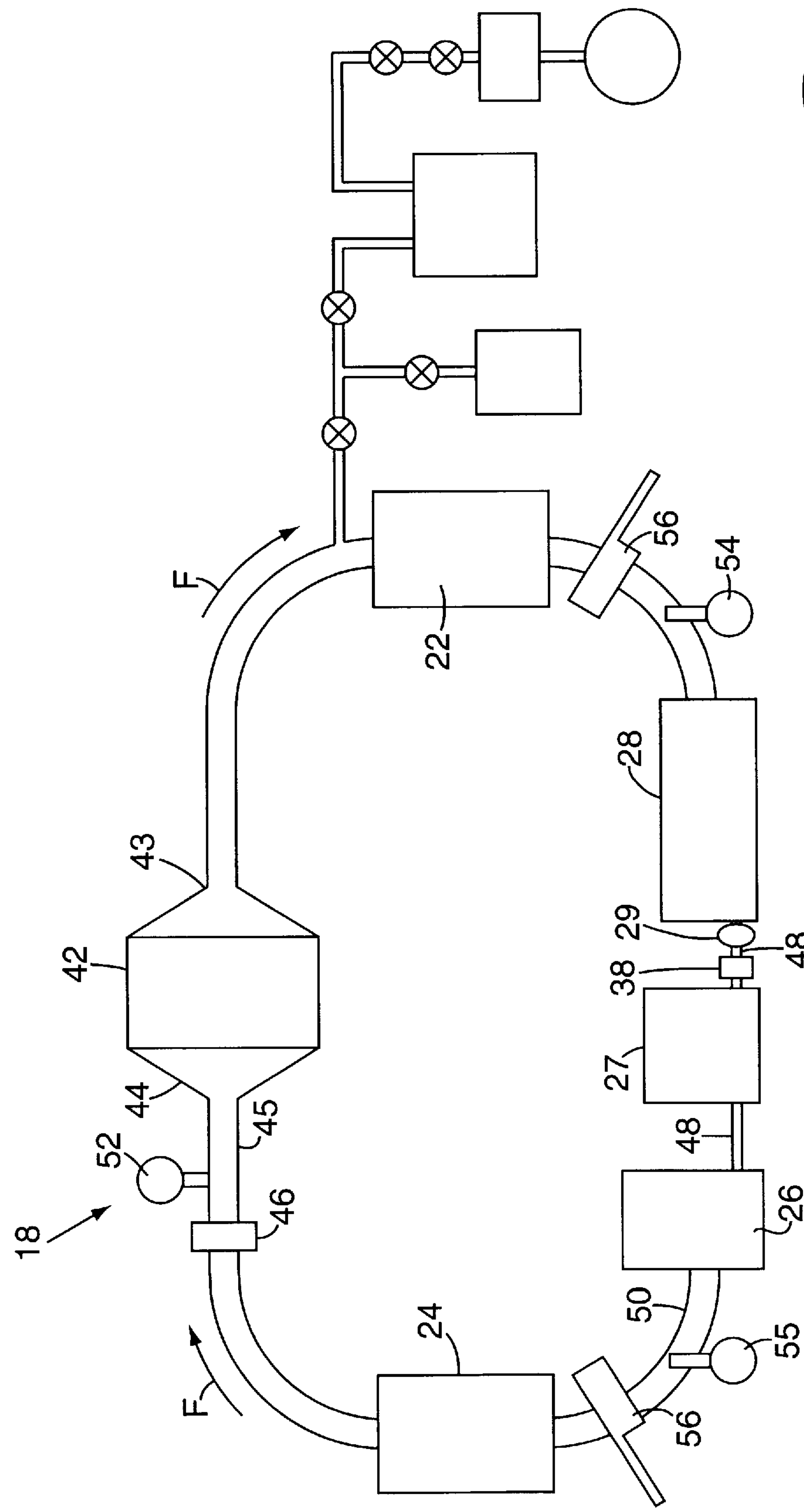

FIG. 5

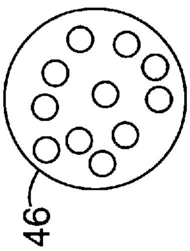

FIG. 5a

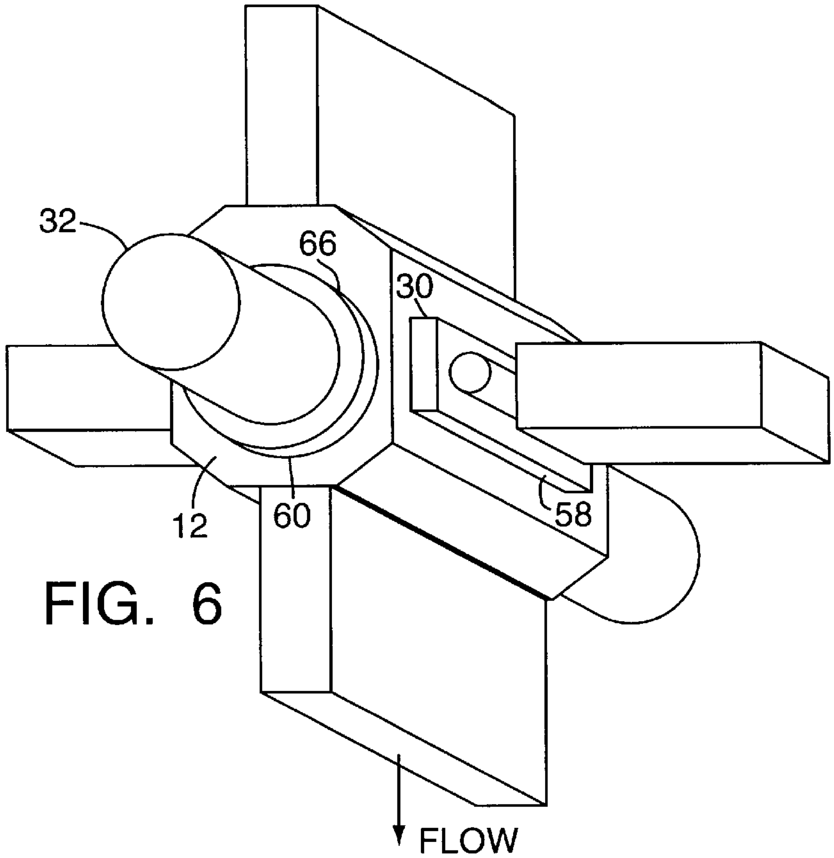

FIG. 6

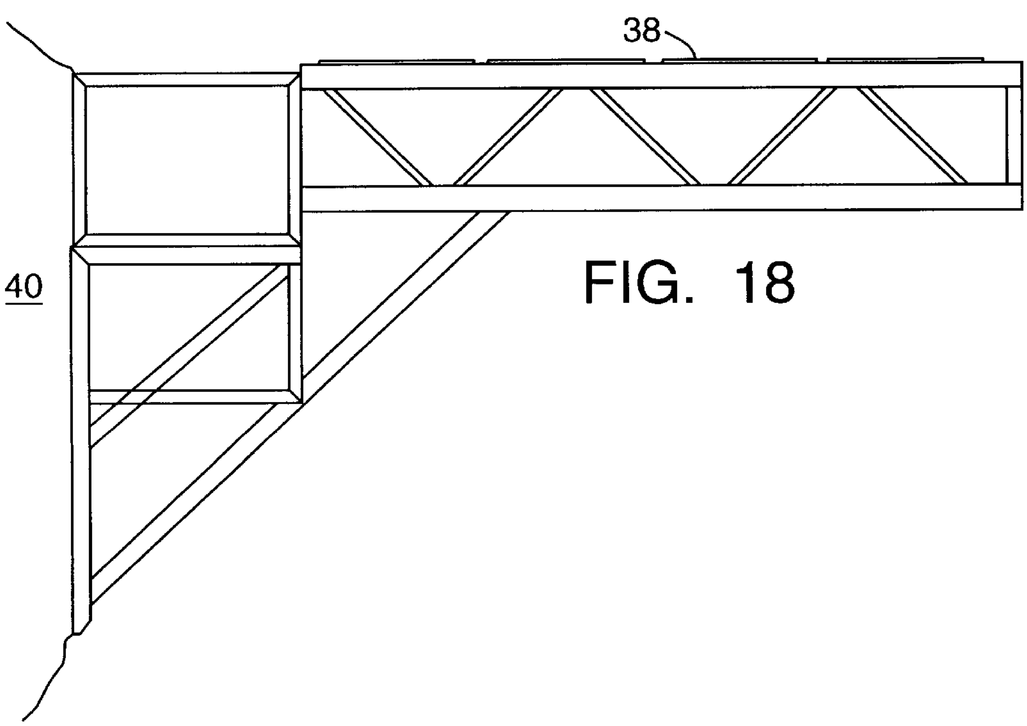

FIG. 18

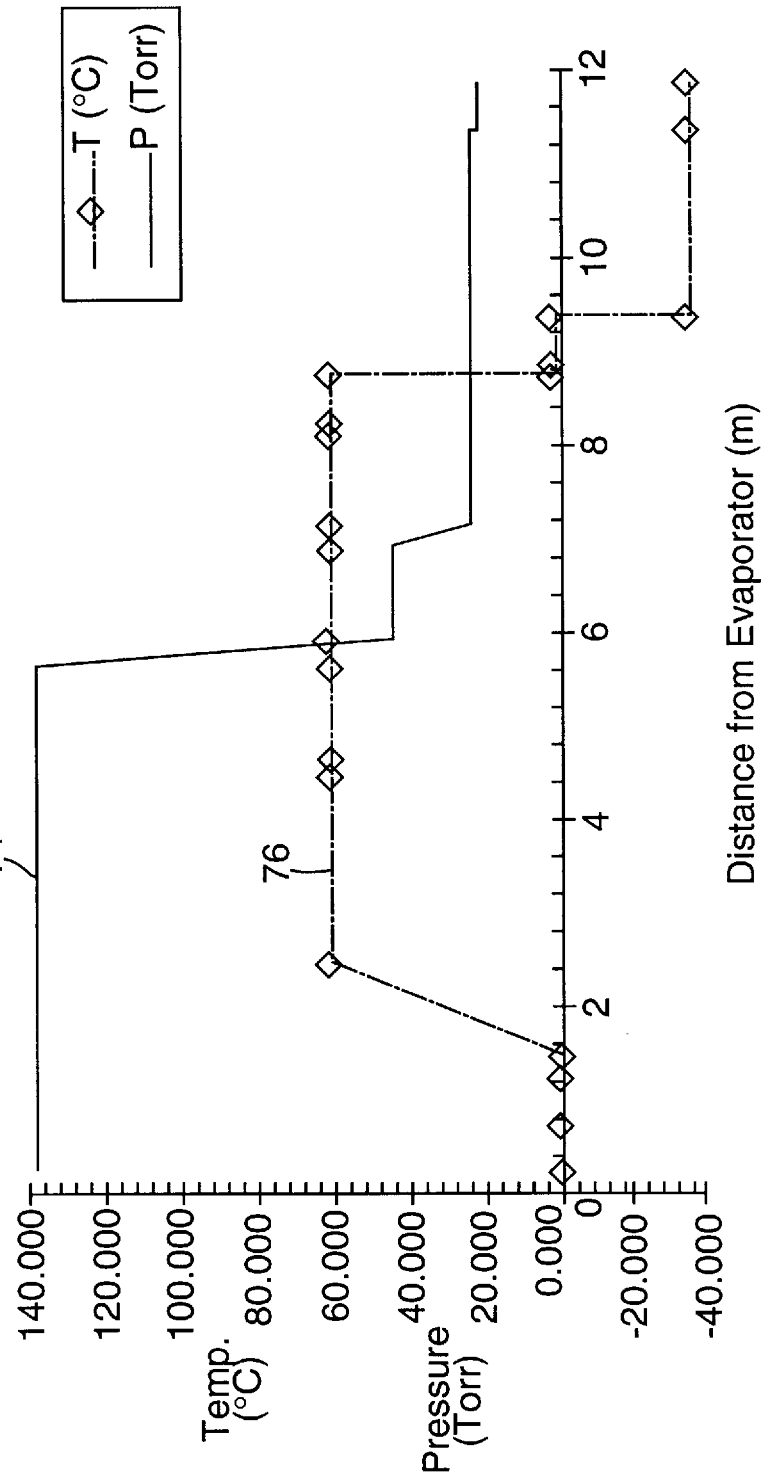
T (°C)
P (Torr)
74
76
Temp. (°C)
Pressure (Torr)
140.000
120.000
100.000
80.000
60.000
40.000
20.000
0.000
-20.000
-40.000
0
2
4
6
8
10
12
Distance from Evaporator (m)

FIG. 7

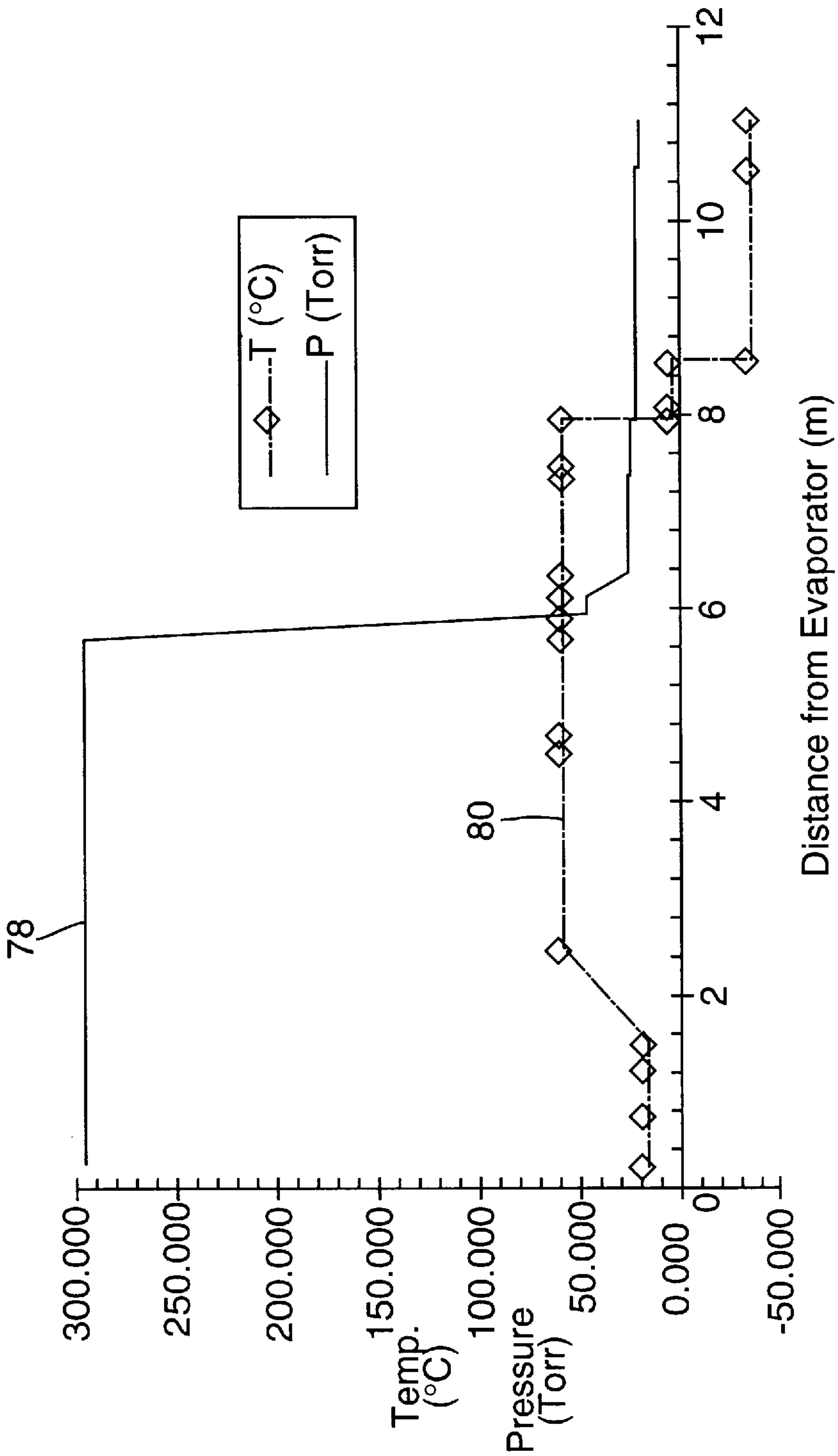
T (°C)
P (Torr)
78
80
Temp. (°C)
Pressure (Torr)
300.000
250.000
200.000
150.000
100.000
50.000
0.000
-50.000
0
2
4
6
8
10
12
Distance from Evaporator (m)

FIG. 8

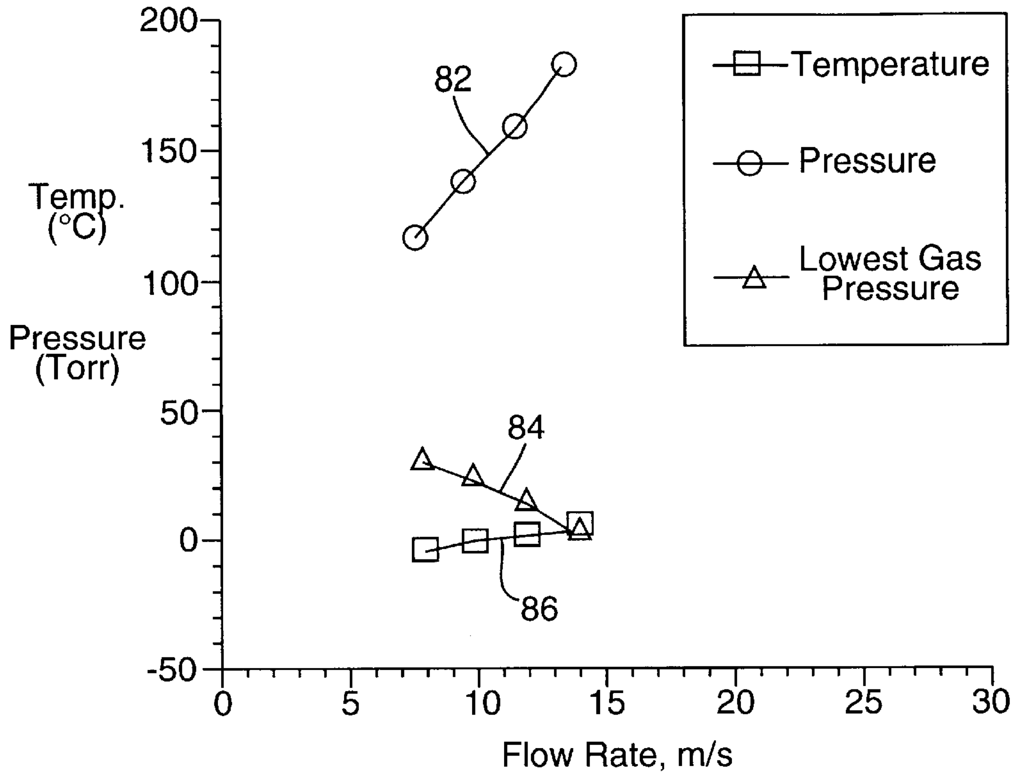
200
150
100
50
0
-50
Temp.
(°C)
Pressure
(Torr)
82
84
86
0
5
10
15
20
25
30
Flow Rate, m/s
Temperature
Pressure
Lowest Gas Pressure

FIG. 9

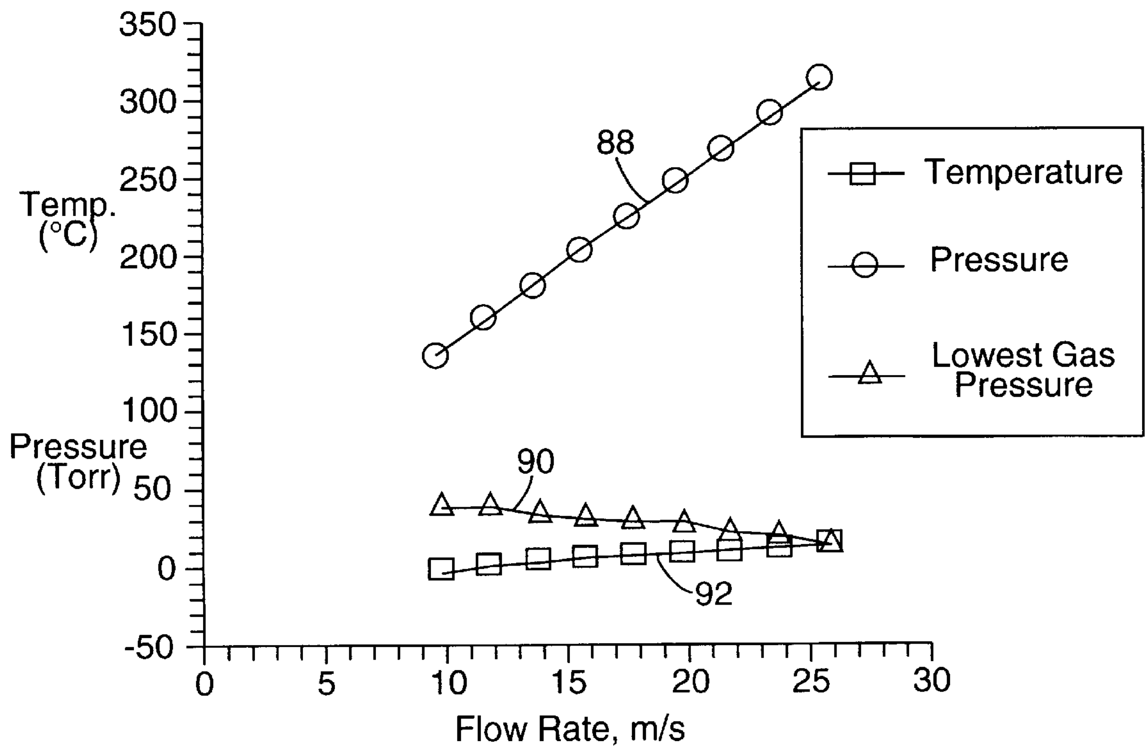
350
300
250
200
150
100
50
0
-50
Temp.
(°C)
Pressure
(Torr)
88
90
92
0
5
10
15
20
25
30
Flow Rate, m/s
Temperature
Pressure
Lowest Gas Pressure

FIG. 10

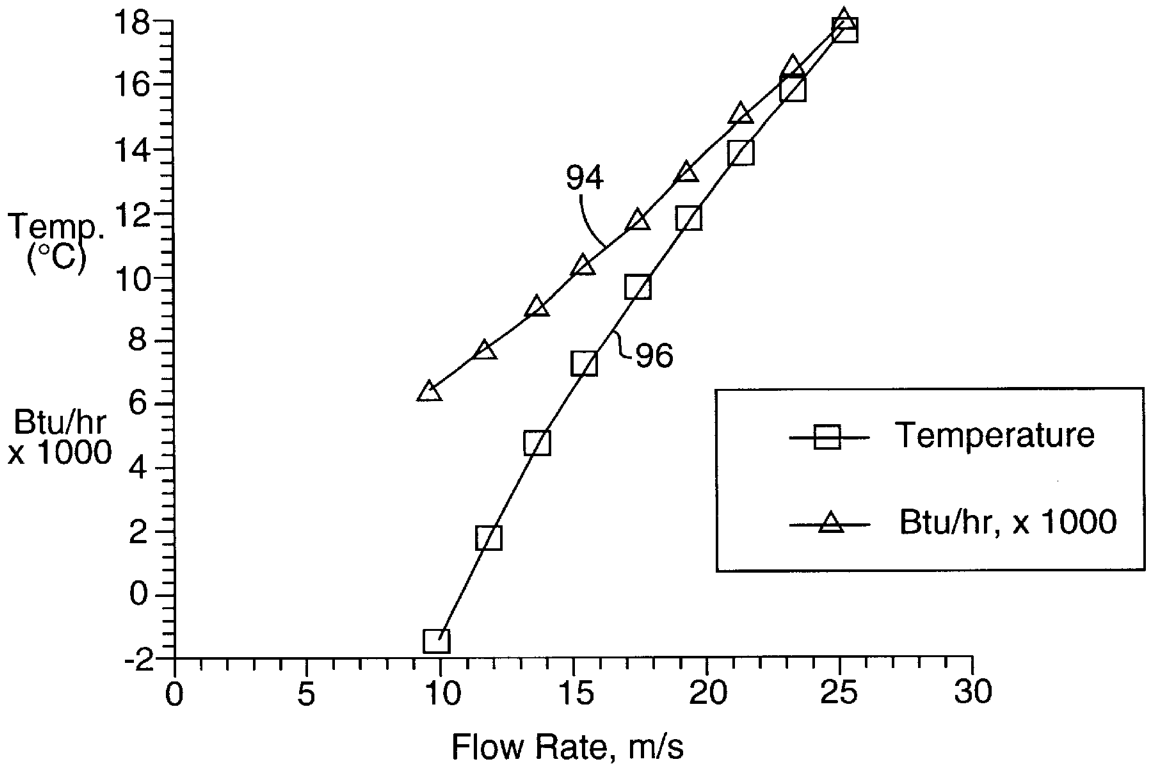

18
16
14
12
10
8
6
4
2
0
-2
Temp. (°C)
Btu/hr x 1000
94
96
Temperature
Btu/hr, x 1000
0
5
10
15
20
25
30
Flow Rate, m/s

FIG. 11

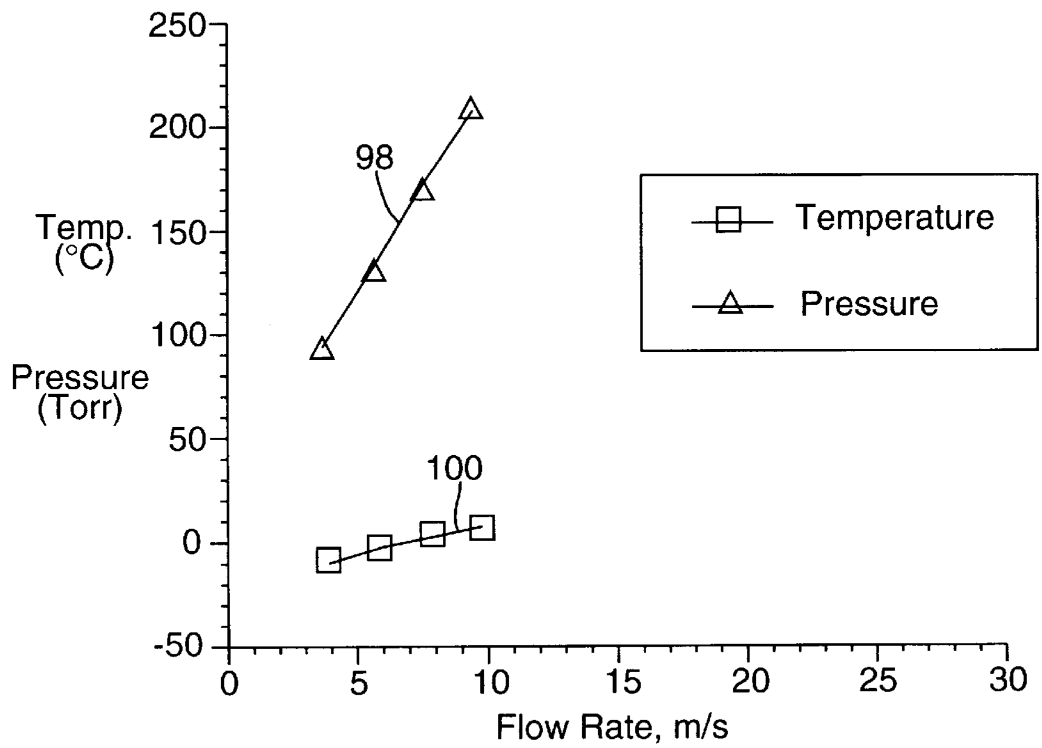

250
200
150
100
50
0
-50
Temp. (°C)
Pressure (Torr)
98
100
Temperature
Pressure
0
5
10
15
20
25
30
Flow Rate, m/s

FIG. 12

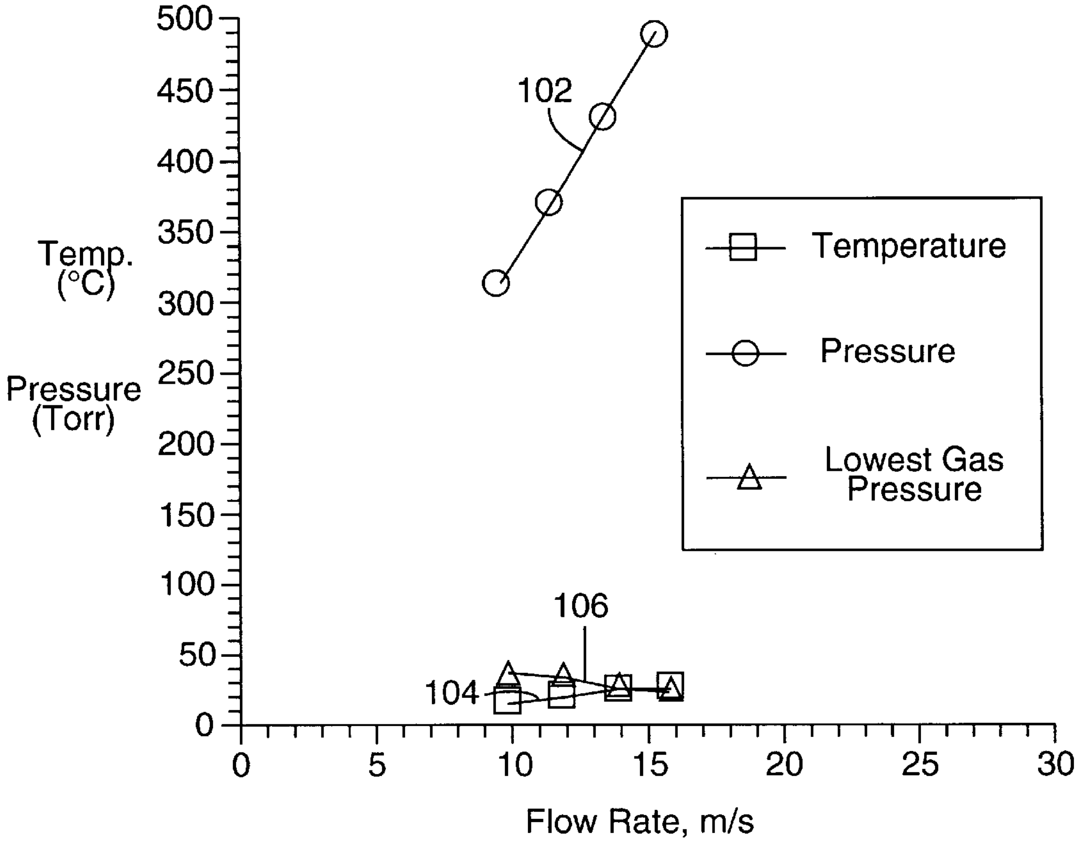
500
450
400
350
300
250
200
150
100
50
0
Temp.
(°C)
Pressure
(Torr)
102
106
104
Temperature
Pressure
Lowest Gas
Pressure
0
5
10
15
20
25
30
Flow Rate, m/s

FIG. 13

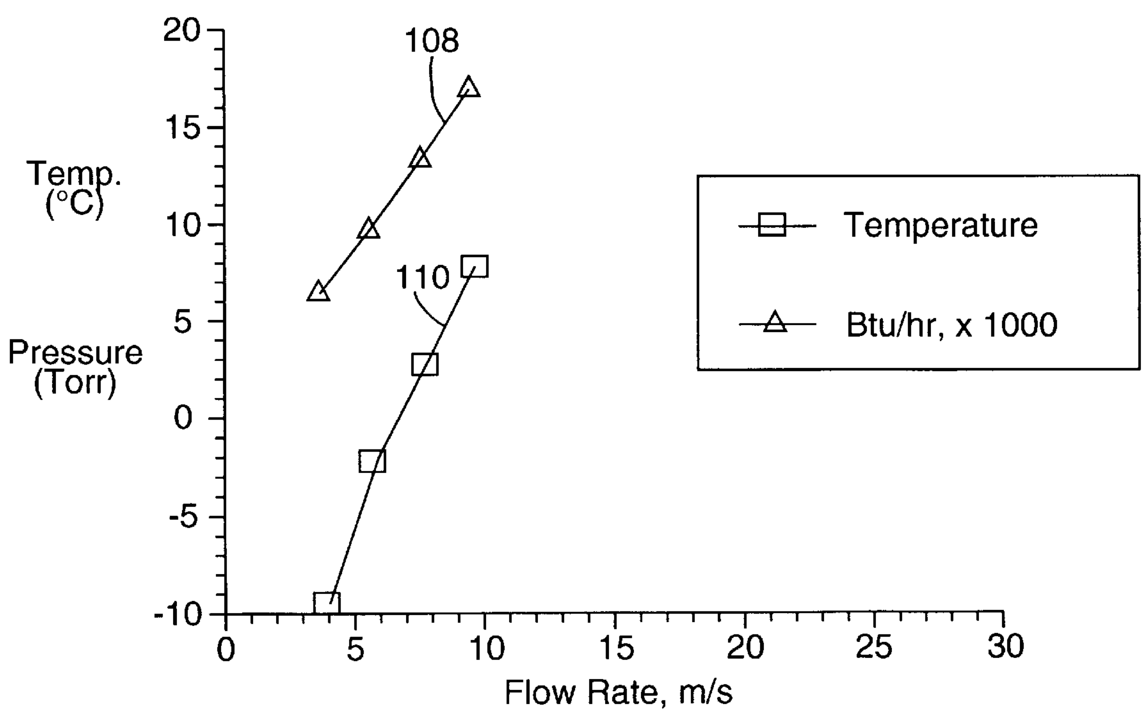
20
15
10
5
0
-5
-10
Temp.
(°C)
Pressure
(Torr)
108
110
Temperature
Btu/hr, x 1000
0
5
10
15
20
25
30
Flow Rate, m/s

FIG. 14

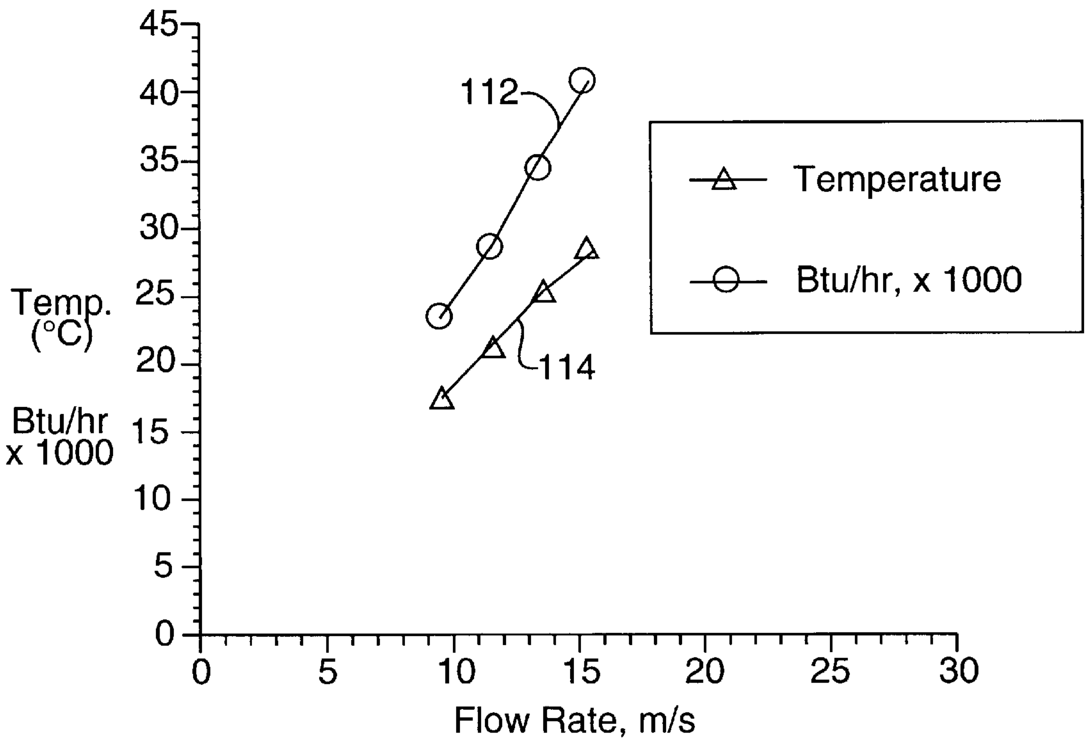

45
40
35
30
25
20
15
10
5
0
Temp. (°C)
Btu/hr x 1000
0
5
10
15
20
25
30
Flow Rate, m/s
112
114
Temperature
Btu/hr, x 1000

FIG. 15

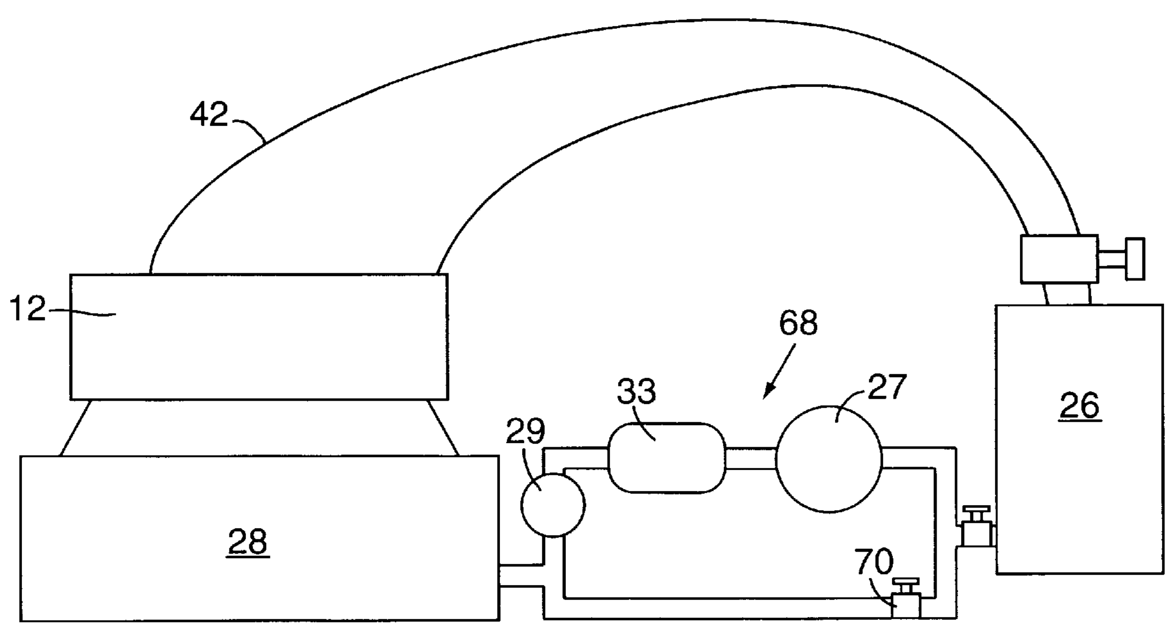

42
12
28
29
33
68
27
26
70

FIG. 16

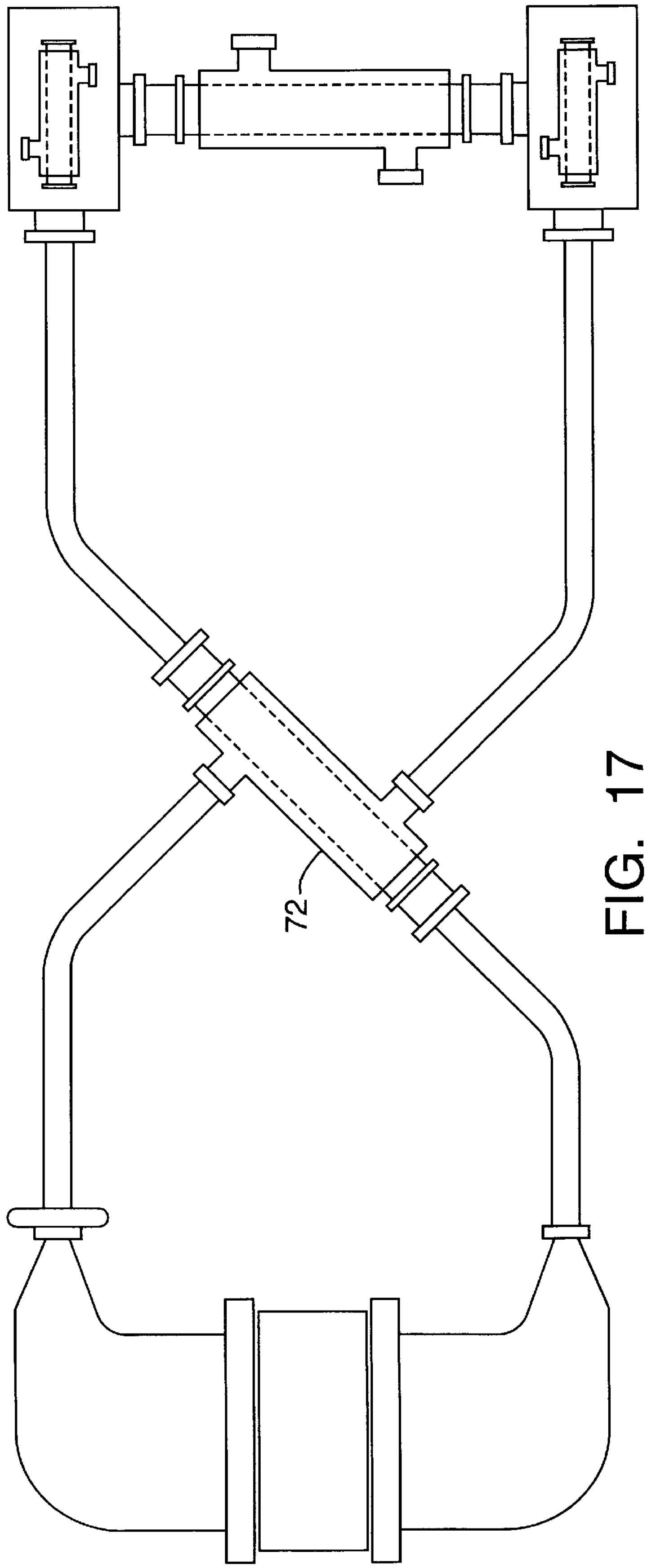

FIG. 17

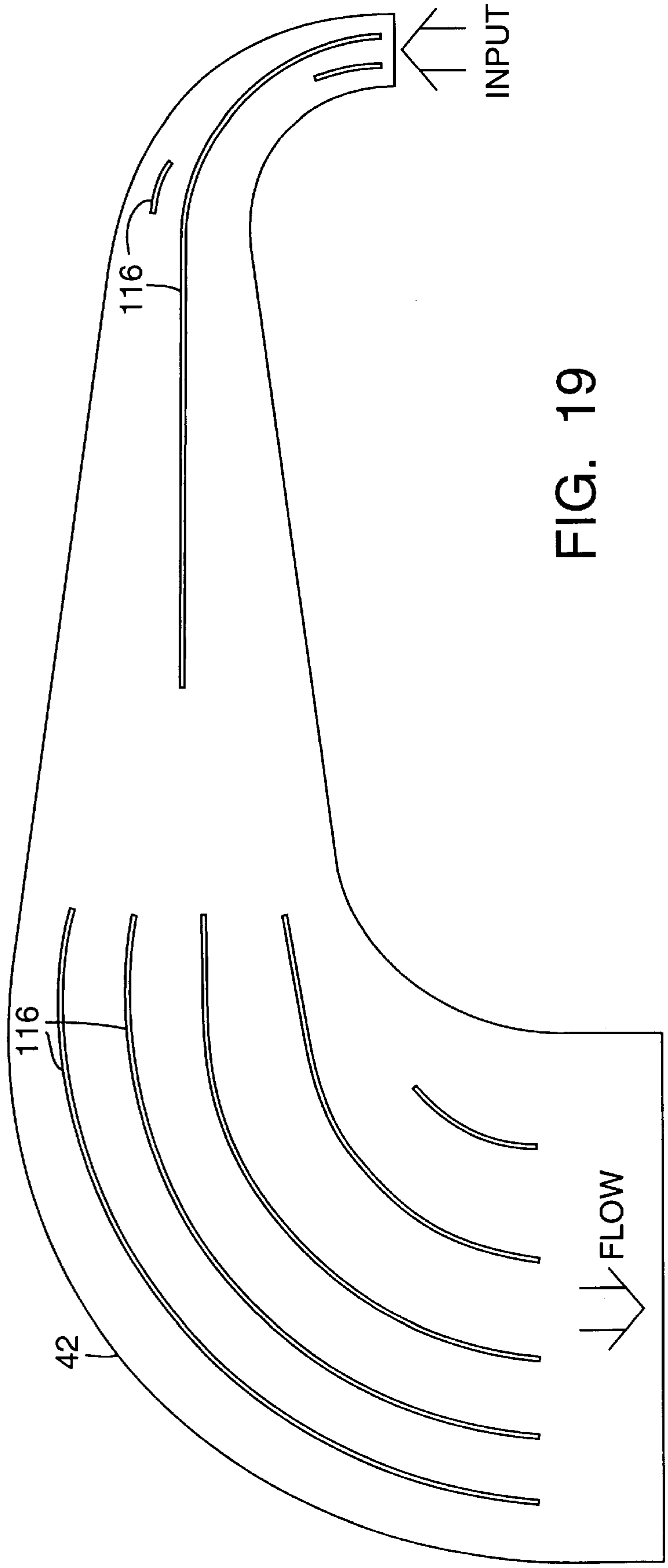

FIG. 19

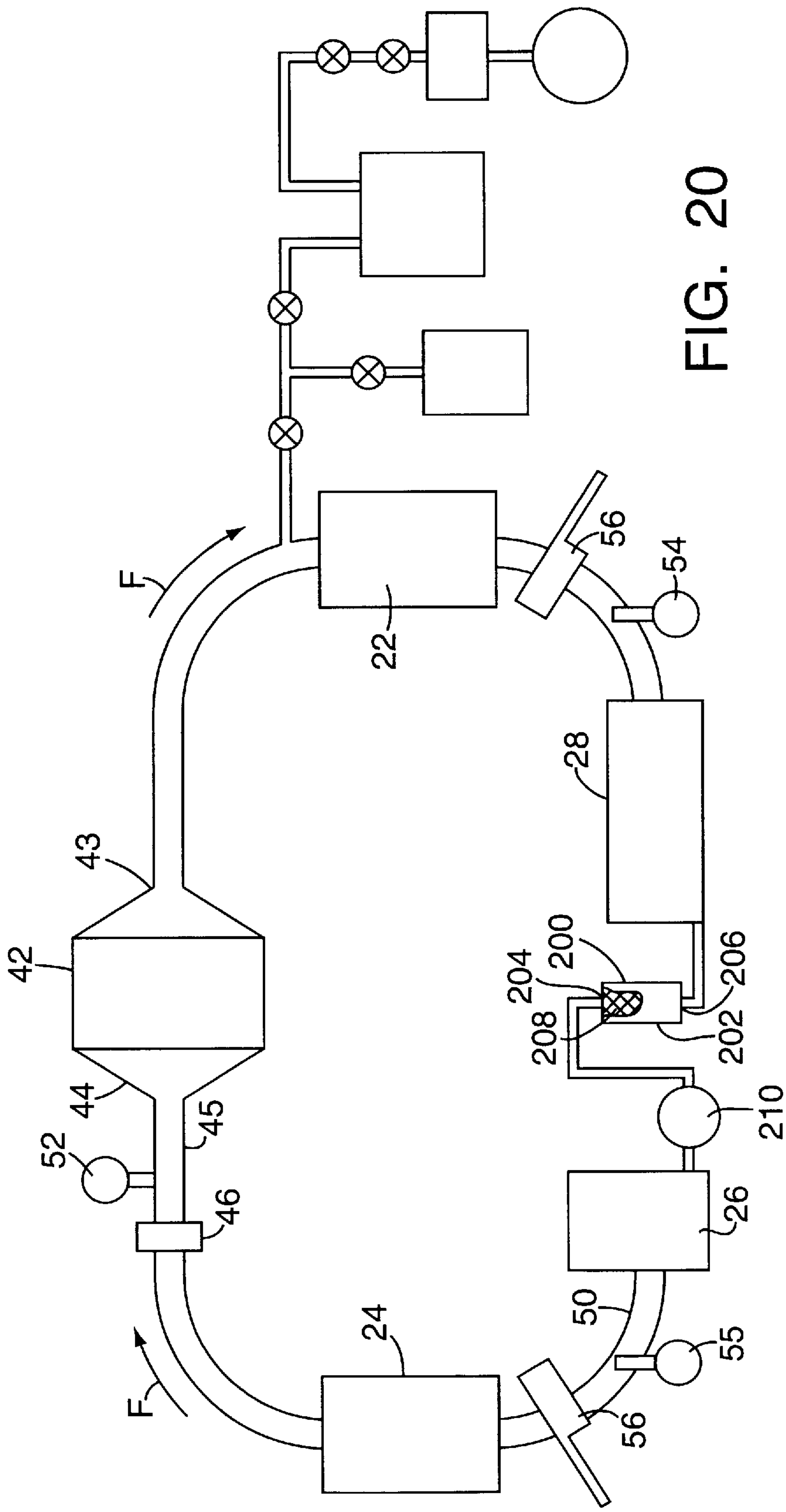
F
22
56
54
28
200
204
206
208
202
210
26
43
42
44
45
52
46
24
50
55
56
F

FIG. 20

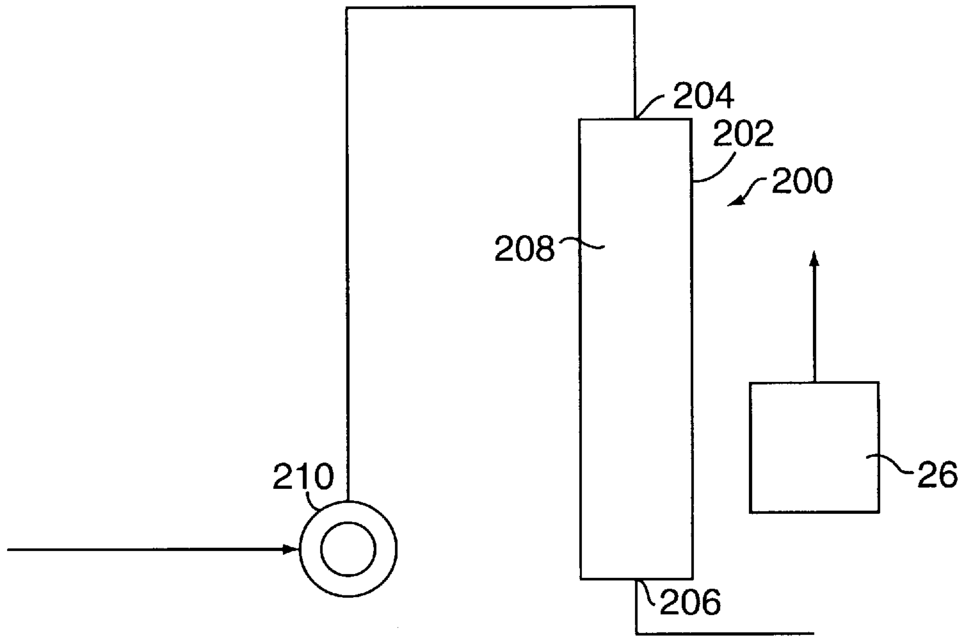

FIG. 21

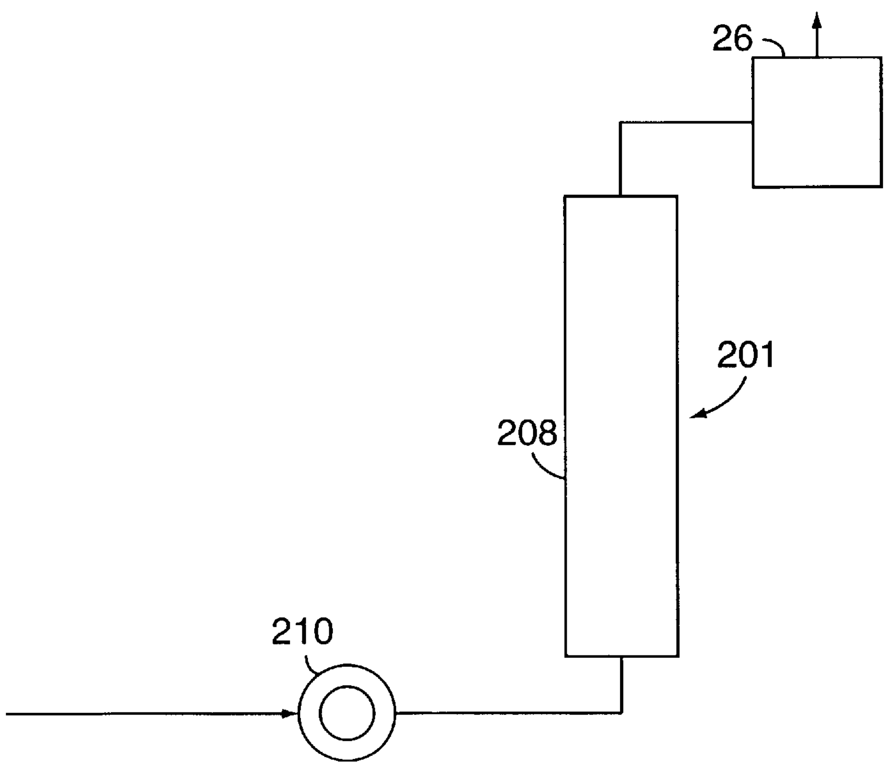

FIG. 23

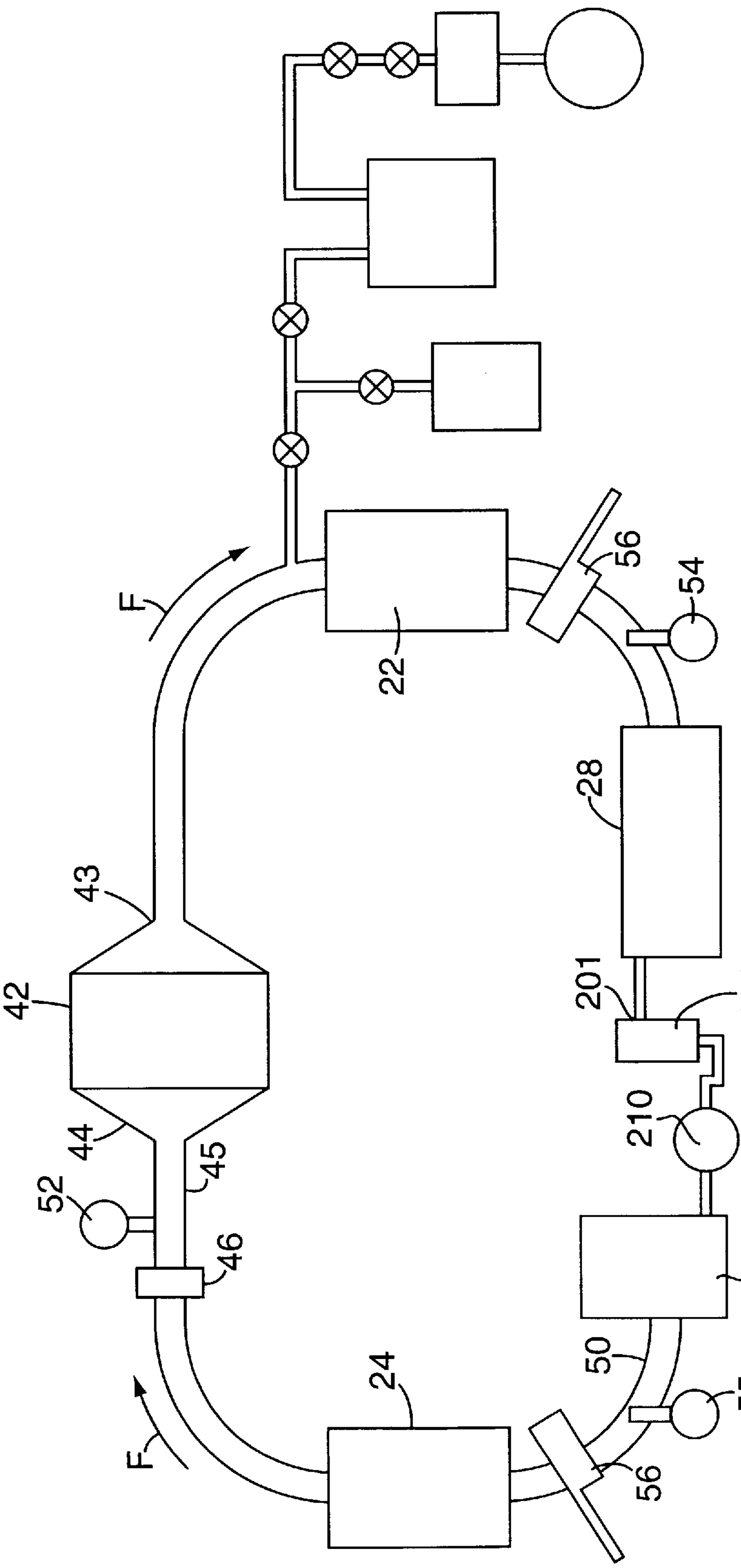

FIG. 22

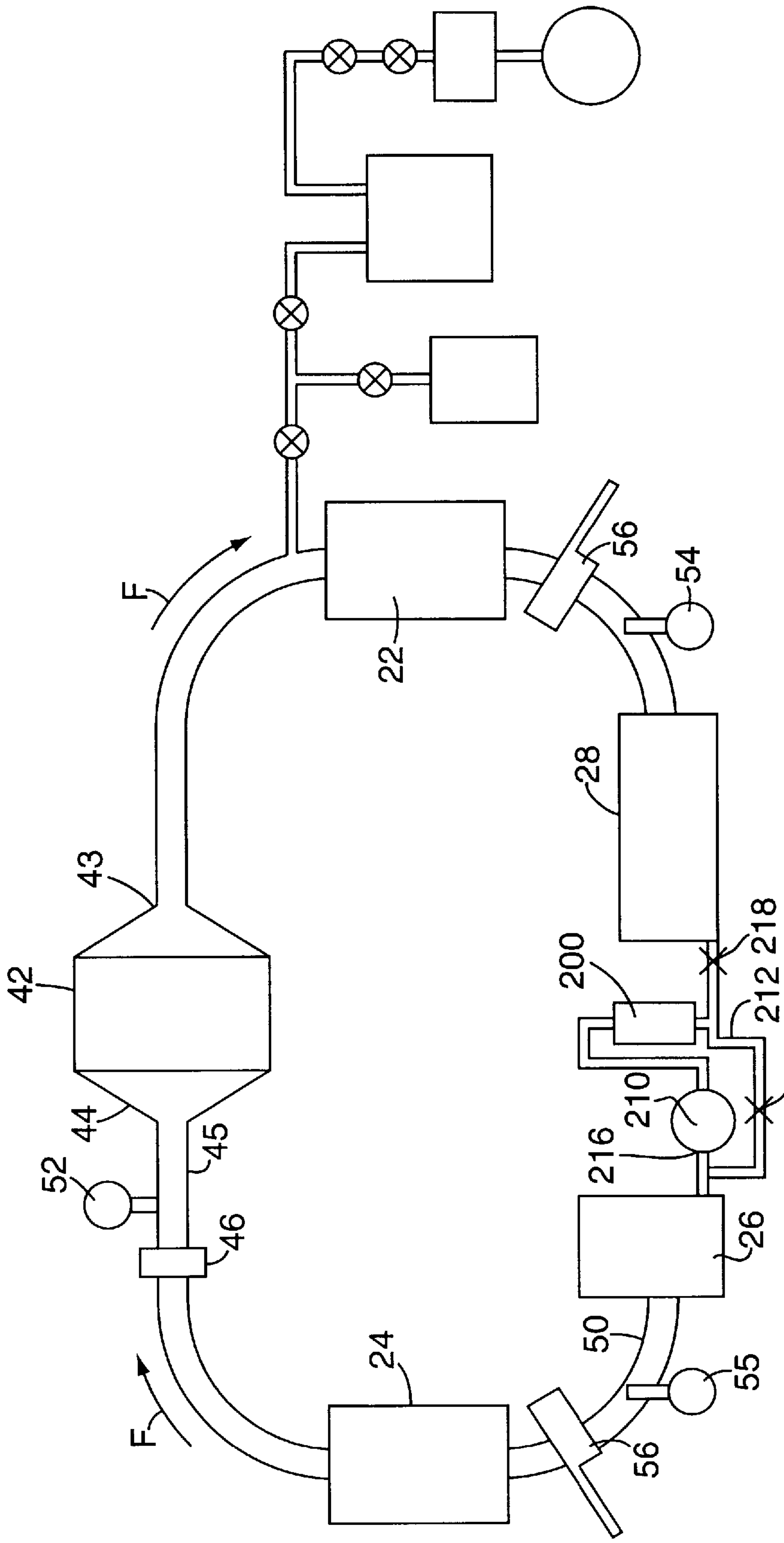
F
22
56
54
28
218
212
218
200
210
216
26
50
55
56
24
F
46
52
45
44
42
43

FIG. 24

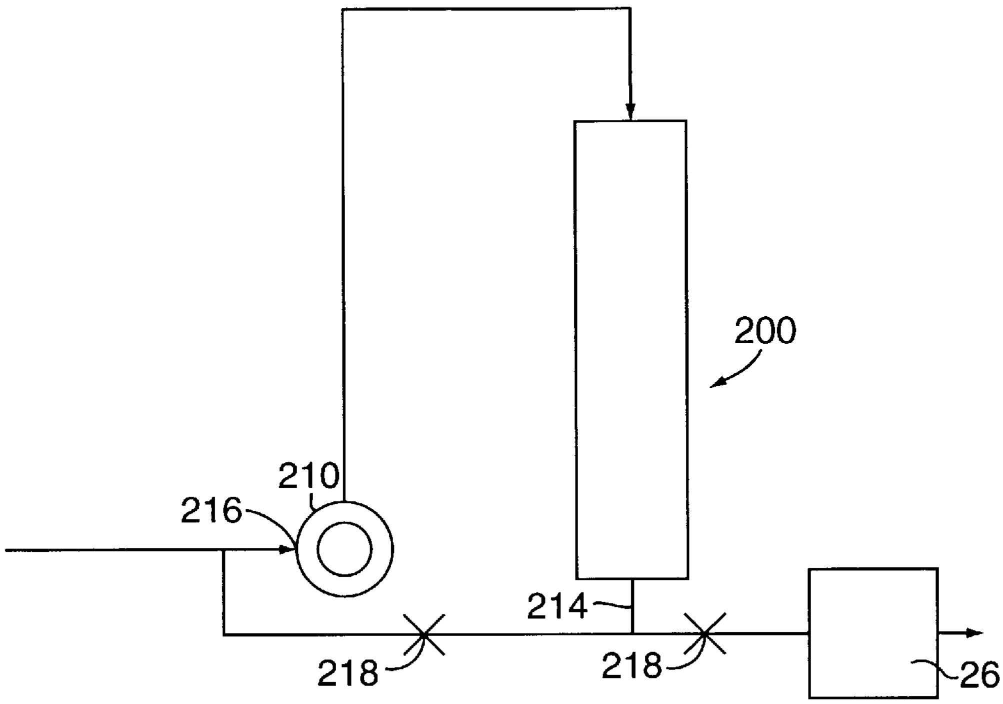

FIG. 25

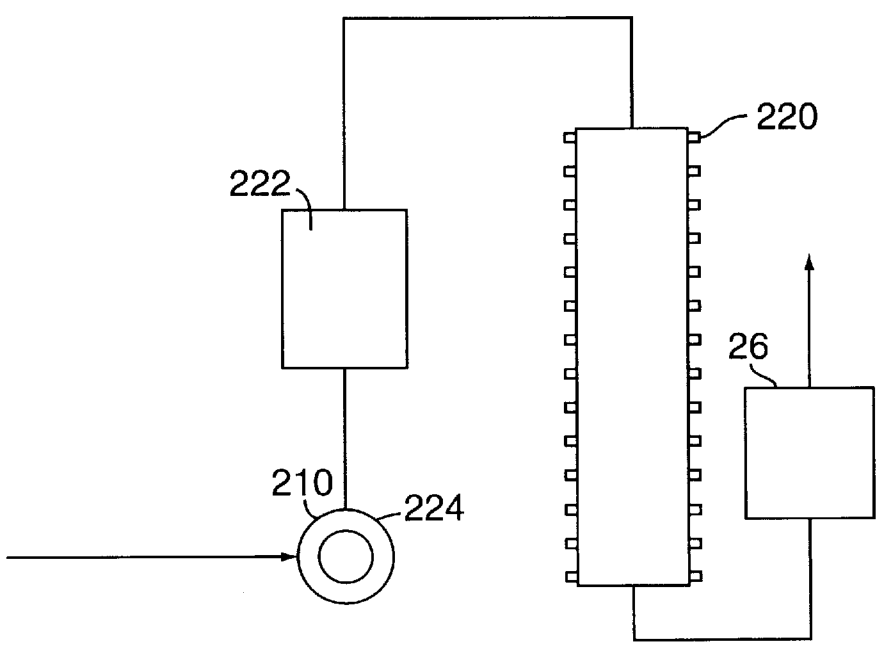

FIG. 27

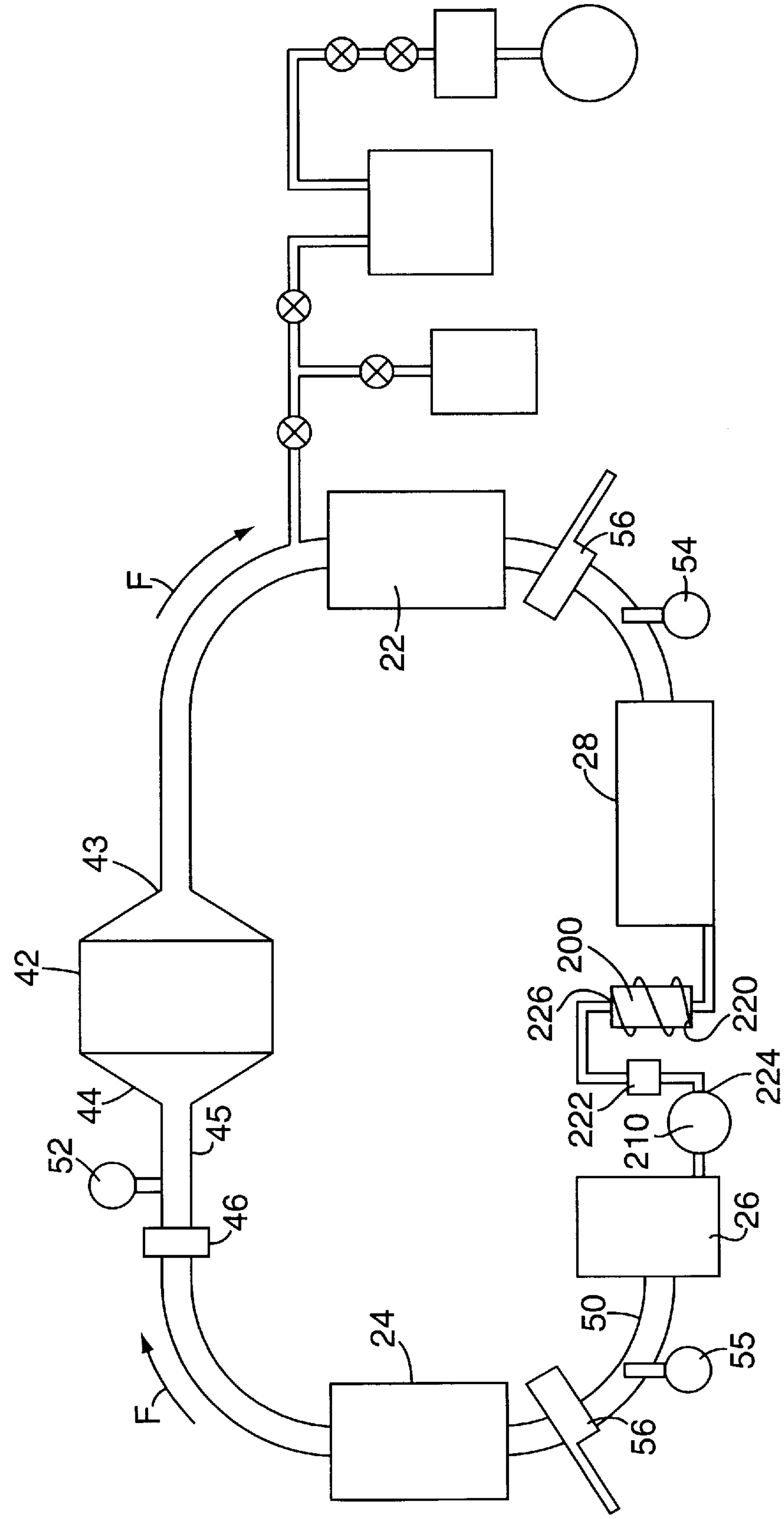
F
22
56
54
28
43
42
200
226
220
222
224
210
44
45
52
46
26
50
55
24
56
F

FIG. 26

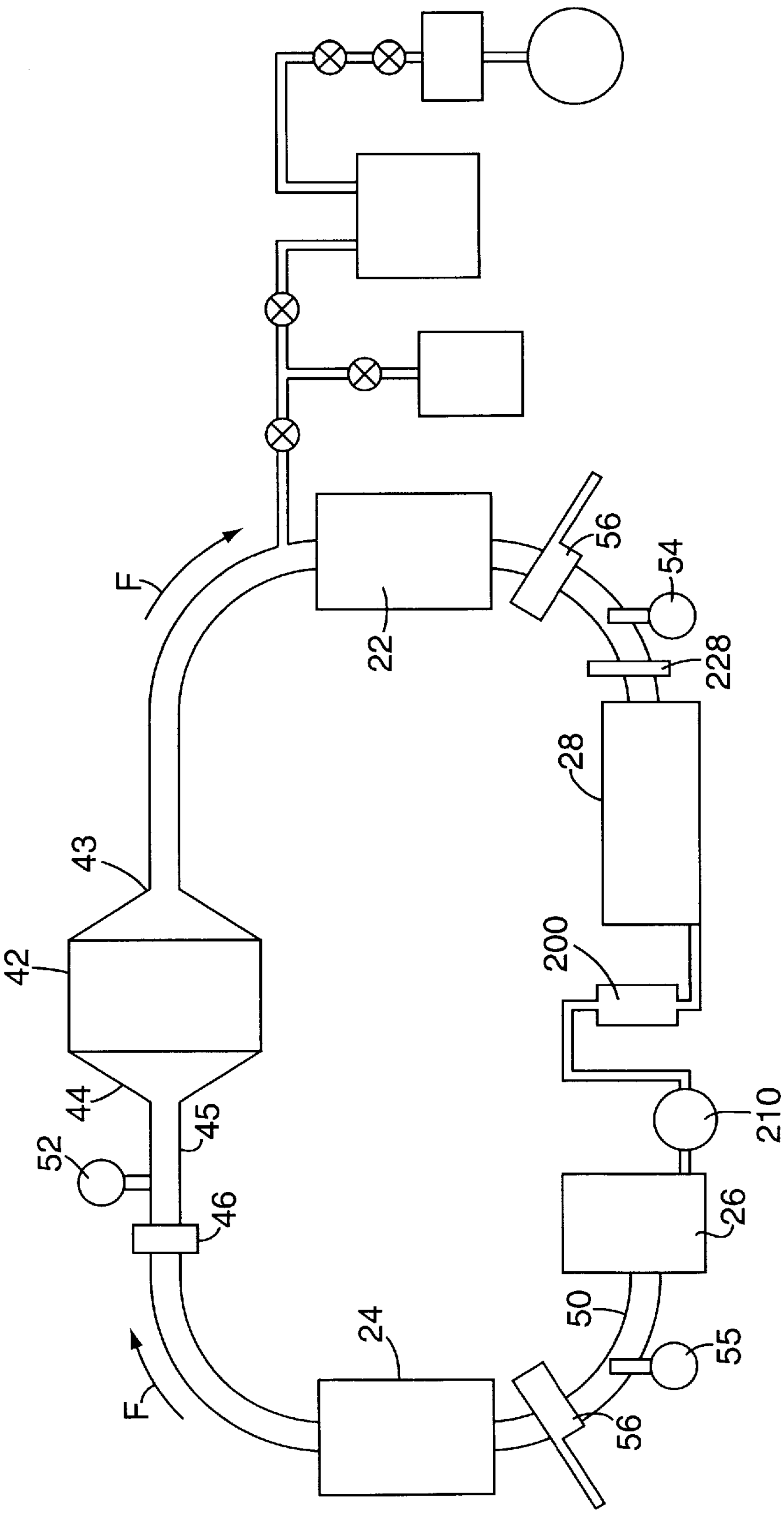

FIG. 28

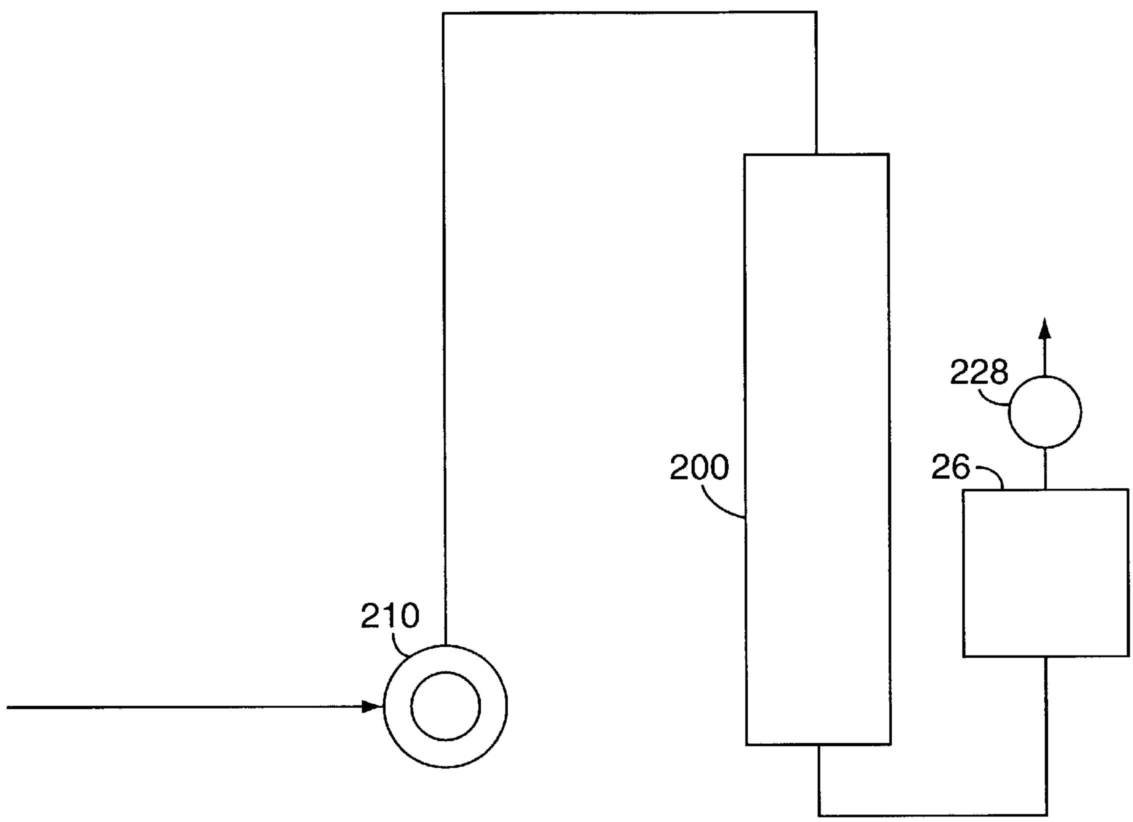

FIG. 29

HIGH POWER PHOTOLYTIC IODINE LASER

This is a CIP of Ser. No. 08/651,471 filed on May 22, 1996 and now U.S. Pat. No. 5,802,093.

This invention was made with government support under contracts (F29601-95C-0043, F29601-96C-0042 and F29601-94C-0073) awarded by the Air Force. The government has certain rights to the invention.

FIELD OF THE INVENTION

This invention relates to the field of Lasers and in particular to continuous wave photolytic iodine lasers.

BACKGROUND OF THE INVENTION

The present invention has particular utility in connection with the industrial, military, and scientific application of lasers and is described herein as applied to such use. In recent years, lasers have been enjoying an ever increasing range of applicability to various processes. The word "laser" is an acronym for "light amplification by stimulated emission of radiation." Therefore, a laser is basically a device for the generation of coherent, nearly single wavelength and frequency, highly directional electromagnetic radiation.

Currently, the gas CO_2 (carbon dioxide), and the solid state Nd:YAG (Yttrium, Aluminum, Garnet) lasers dominate the material cutting and welding industries. However, the applicability of these lasers in a wide variety of manufacturing processes is limited. The gas CO_2 laser, because of the beam's long wavelength, and the Nd:YAG laser because of its low brightness, both require a great deal of power to be useful. Brightness, also called the beam quality compares the relative amount of energy within the central lobe of a laser beam with that of a perfect laser beam. The numbers corresponding to brightness are greater than or equal to unity, with values of 1 indicating superior brightness and values much greater than 2 or 3 indicating poor performance.

Due to its high brightness and small wavelength, the photolytic iodine laser (PIL) has the potential to address the needs of a wide variety of markets. The PIL is a gas laser which employs a gas as a fuel for generating the laser beam. Usable PILs were first developed in the early **1980**'s. However, these early PILs were not suitable for manufacturing processes. They displayed poor output power as compared to input power, as well as poor repeatability of performance. Additionally, these early systems were prone to excessive buildup of molecular iodine which severely interrupted the lasing process.

PILs require a continuous flow of fuel through the laser's gain cell region in order to generate a laser beam. The laser's gain cell is that section of the laser where light amplification occurs. For a given gain cell size, the laser's power is proportional to the flow rate of the gaseous fuel through the gain cell. Conventional PILs have employed blowers in the fuel delivery system to provide adequate fuel flow rates. However, these blowers can be costly. In addition, it has been found that merely increasing the pressure in the system is not sufficient. The types of fuel employed in PILs, namely C_3F_7I, exhibit high frictional properties which basically cause the fuel to "stick" to the walls of the conduits within which the fuel flows. This results in significant pressure drops in the fuel system thereby making it difficult to establish and maintain fuel flow rates sufficient to generate a laser beam of proper intensity.

PILs employ microwave systems to provide power to the lamps needed to generate a laser beam. In the past, these systems utilized low power magnetrons as the power source. Therefore, these systems required large numbers of magnetrons; one for each lamp, and extensive supporting systems, to provide for adequate laser power. The microwave systems were very complex and required a great deal of maintenance. This made these lasers impractical for industrial use.

Therefore, it is important to provide a PIL whereby the components are kept simple, and the number of components is kept to a minimum. This will allow for ease of maintenance, as well as make the laser more competitive with conventional material processing equipment.

In view of the foregoing, there is a current need and large market potential for an economical materials processing laser which is superior in both brightness, and processing performance to those currently in use. Moreover, the laser must be capable of maintaining its performance integrity over extended periods of time.

Therefore, the general object of the present invention is to provide a continuous wave laser for use in industrial applications which can be economically procured and operated, yet is capable of generating a laser beam of sufficient power so as to be practical.

It is a further object of the present invention to provide a CW PIL which does not require the use of expensive blowers to maintain the fuel flow rate.

It is yet another object of the present invention to provide a PIL wherein the microwave system is capable of powering more than one lamp on a single magnetron.

It is still a further object of the present invention to provide a method for determining critical laser parameters.

SUMMARY OF THE INVENTION

The present invention meets these and other objects by providing a continuous wave photolytic iodine laser (CW PIL) which employs a gain cell for receiving a continuous supply of gaseous fuel. The gain cell has an optical axis and a lamp positioned along the axis. Additionally, the gain cell includes beam transfer optics, a gain cell inlet and outlet, and a laser resonator for shaping a laser beam. A microwave subsystem is also provided, and is in communication with the gain cell for driving the lamp such that a laser gain medium is pumped through the gain cell. The CW PIL incorporates a closed loop fuel system for supplying a continuous flow of gaseous fuel to the gain cell. The fuel system has a fuel inlet member in communication with the gain cell inlet for receiving and presenting the gaseous fuel to the gain cell, a condenser is in communication with the gain cell exit for converting the gaseous fuel into a liquid, a scrubber is provided for removing molecular iodine (I_2) and any by-products of the lasing operation from the liquefied fuel thereby purifying and preparing the fuel for recycling back to the gain cell. A pump is interposed between the condenser and the scrubber to transport and pressurize the liquefied fuel. An evaporator is in communication with the scrubber for receiving and converting the purified liquid fuel to a gas, thereby causing an increase in the closed loop fuel system's pressure which forces the gaseous fuel through the gain cell at a flow rate whereby substantially all of the molecular iodine and any lasing by-products are swept out of the fuel cell.

According to another aspect of the present invention, the photolytic iodine laser includes a fuel control system having a controller for regulating the flow of the gaseous fuel through the laser. The fuel control system includes apparatus for generating concentration signals corresponding to a rate of change in concentration of excited iodine (I^*) in the fuel characterized by,

$$\int_{t1}^{t2} dI^* = \int_{t1}^{t2} 2\sigma_{pump}F_{uv}(RI)dt - \int_{t1}^{t2} 2k_1 + (I^*)(I_2)dt - \int_{t1}^{t2} 2\sigma_{se}F_{IR}(I^*)dt - \int_{t1}^{t2} k_8(I^*)(RI)dt$$

as well as apparatus for receiving these concentration signals and then generating molecular iodine concentration signals for adjusting the rate by which the concentration of molecular iodine (I_2) in the gaseous fuel changes as the fuel passes through the closed loop fuel system in accordance with a three body deactivation reaction provided by,

$$\left(\frac{\partial I^*}{\partial t}\right) = k_{13}(I^*)(I)(I_2),$$

and

$$\int_{t1}^{t2} dI_2 = \int_{t1}^{t2} k_{12}(I^*)(RI)dt.$$

The fuel control system further includes apparatus for receiving iodine concentration signals and generating correction signals to adjust the molecular iodine (I_2) concentration for a linear fuel flow velocity due to a resultant decrease in the concentration of steady state (I_2), as characterized by,

$$(I_2)_{corrected} = (I_2) - \frac{I_2(1\text{cm})_{gain\ cell}}{\text{Flow Rate (cm/}s)}\,\Delta t.$$

The correction signals are received by the apparatus and gain signals for controlling the small signal gain of the laser due to a population inversion of the excited state atomic iodine (I^*) to a ground state (I) are generated by the apparatus as provided by,

$$\alpha = \frac{\left(N_2 - \frac{g_u}{g_l}N_1\right)\lambda^2\eta g(v)}{8\pi n^2 t_{spont}},$$

where

$$\eta = \frac{\epsilon}{\epsilon_0},\ t_{spont} = \frac{1}{A_{spont}},$$

and

$$\frac{g_u}{g_l} = 0.5.$$

The gain signals are then received the fuel control system and based on their values, intensity signals corresponding to the circulating intensity of the resonator are generated, thereby controlling the magnitude of the infrared flux necessary for regulation of the stimulated emissions from the laser. These intensity signals are provided by,

$$I_{out} = \frac{I_{sat}}{\left(1 + \frac{r1}{r2}\right)(1 - r1r2)}\left[2\alpha_{mo}L - \ln\frac{1}{r1r2}\right]$$

where r_1 and r_2 are the e field reflectivities, and R_1 and R_2 are the ϵ^2, or power reflectivities, α_{mo} is the small signal gain, L is the single pass length of the gain, and I_{sat} is the saturation intensity of the laser where,

$$R_1 = r_1^2$$

in delta notation, the transmission and reflectivities are related by,

$$R_1 = 1 - \delta_1 = T_1$$

and

$$R_2 = 1 - \delta_2 = T_2,$$

the total loss of the resonator is represented by $\delta_c = \delta_0 + \delta_1 + \delta_2$ where the linear gas absorption loss, δ_0, is assumed to be zero.

Once the intensity signals have been received, mirror loss correction signals that compensate for losses associated with the mirrors in the resonator optics are generated by the apparatus. The mirror loss correction signals are evidenced by,

$$\delta_c = \ln\frac{1}{R_i} = 2\ln\frac{1}{r_i} \approx \ln\frac{1}{R_1R_2}\ \text{or,}$$

$$\delta_c = 2\alpha_0 p + \ln\frac{1}{R_1R_2} \approx \ln\frac{1}{R_1R_2}.$$

The fuel control system includes apparatus for receiving the mirror loss signals and generating loaded gain control signals for controlling the loaded gain, α_m, resulting from a homogeneous broadening as provided by,

$$\alpha_m = \alpha_{m0} + \frac{1}{1 + \frac{1}{I_{sat}}},$$

where α_m is the gain per cm and pm is the single pass gain length, are generated.

According to still another aspect of the present invention, a heat transfer control system for regulating the rate of heat transfer from and to the gaseous fuel is provided. The heat transfer control system includes apparatus for generating heat transfer signals corresponding to a rate at which heat is transferred through the tubing walls of heat exchangers. These heat transfer control signals are characterized by,

$$\dot{Q} = \bar{U}A\Delta T_m.$$

The apparatus receives the heat transfer signals, and generates phase change signals determined by a sensor that senses the rate at which the fuel passes through and changes phase in the condenser. These phase change signals are provided by,

$$\dot{Q} = \dot{m}h_{vap};$$

where h=enthalpy. The phase change signals are received by the apparatus and evaporation rate signals for controlling the rate at which heat is transferred to the fuel as it passes through the evaporator are generated by the apparatus. This rate is evidenced by,

$$\dot{Q} = \dot{m}\Delta h.$$

The evaporation rate signals are received by the apparatus, and major loss compensation signals are generated to account for any major losses due to friction in the pipes and conduits in the system. These major losses are characterized by,

$$h_{loss} = f\left(\frac{L}{D}\right)\frac{V^2}{2g}$$

(head loss);
where the friction f is given by,

$$f = \left[1.14 - 2\log\left(\frac{\epsilon}{D} + \frac{21.25}{Re^{0.9}}\right)\right]^{-2}$$

(ϵ=the pipe's surface roughness};
In addition to the major losses, minor losses must also be accounted for. Therefore, minor loss signals are generated by the apparatus as characterized by,

$$h_{loss} = K\frac{V^2}{2g};$$

and
The major and minor loss signals are combined by the apparatus such that pump control signals can be generated to control the amount of work done by a pump on the fuel, and to optimize the pump efficiency as determined by;

$$-\frac{dW_{shaft}}{dt} = \rho Q[U_{out}V_{tout} - U_{in}V_{tin}];$$

and

$$\left[\frac{p_2}{\gamma} + \frac{V_2^2}{2g} + Z_2\right] = \frac{e_{pump}}{g}\left[\vec{U}_2 \cdot \vec{V}_2 - \vec{U}_1 \cdot \vec{V}_1\right] + \left[\frac{p_1}{\gamma} + \frac{V_1^2}{2g} + Z_1\right]$$

In an alternate embodiment, an elongated rectangular gain cell is incorporated into a CW PIL provided by the present invention.

In another embodiment of the present invention, a first heat exchanger is interposed between the gain cell exit and the condenser for pre-cooling the fuel, and a second heat exchanger is interposed between the evaporator and the fuel inlet member to pre-heat the gaseous fuel as it comes out of the evaporator.

In yet another embodiment of the present invention, a cross flow heat exchanger replaces the first and second heat exchangers.

BRIEF DESCRIPTION OF THE DRAWINGS

These and other features, aspects, and advantages of the present invention will become better understood with regard to the following description, appended claims, and accompanying drawings where:

FIG. **1** is a schematic illustration of a CW PIL as provided by the present invention.

FIG. **2** is a simplified schematic illustration of the microwave subsystem of the CW PIL of FIG. **1**.

FIG. **2***a* is a simplified schematic illustration of the microwave cavity of the CW PIL of FIG. **1**.

FIG. **3** is a simplified schematic illustration of the gain cell of the CW PIL of FIG. **1**.

FIG. **4** is a diagrammatic illustration showing the relationship between the fuel pressure in the gain cell versus the temperature in the condenser for the CW PIL of FIG. **1**.

FIG. **5** is a simplified schematic illustration of the closed loop fuel system of the CW PIL of FIG. **1**.

FIG. **5***a* is a front view of the orifice plate of the CW PIL of FIG. **1**.

FIG. **6** is a simplified schematic of the gain cell of the CW PIL of FIG. **1**.

FIG. **7** is a diagrammatic illustration showing the relationship between the distance from the evaporator and the temperature and pressure in the closed loop fuel system of the CW PIL of FIG. **1**.

FIG. **8** is a diagrammatic illustration showing the relationship between the distance from the evaporator and the temperature and pressure in the closed loop fuel system of the CW PIL of FIG. **1**.

FIG. **9** is a diagrammatic illustration showing the relationship between the fuel flow rate versus, the evaporator temperature, and the evaporator and condenser pressures for a closed loop fuel system of the CW PIL of FIG. **1**.

FIG. **10** is a diagrammatic illustration showing the relationship between the fuel flow rate versus, the evaporator temperature, and the evaporator and condenser pressures for a closed loop fuel system of the CW PIL of FIG. **1**.

FIG. **11** is a diagrammatic illustration showing the relationship between the fuel flow rate versus evaporator temperature, and the heat removed by the evaporator for a closed loop fuel system of the CW PIL of FIG. **1**.

FIG. **12** is a diagrammatic illustration showing the relationship between the fuel flow rate versus temperature, and pressure for a closed loop fuel system having an orifice plate of the CW PIL of FIG. **1**.

FIG. **13** is a diagrammatic illustration showing the relationship between the fuel flow rate versus the evaporator pressure, the lowest gas pressure, and the evaporator temperature for a closed loop fuel system of the CW PIL of FIG. **1**.

FIG. **14** is a diagrammatic illustration showing the relationship between the fuel flow rate versus evaporator temperature, and the heat removed by the evaporator for a closed loop fuel system having an orifice plate of the CW PIL of FIG. **1**.

FIG. **15** is a diagrammatic illustration showing the relationship between the fuel flow rate versus evaporator temperature, and the heat removed by the evaporator for a closed loop fuel system having an orifice plate of the CW PIL of FIG. **1**.

FIG. **16** is a simplified schematic illustration showing an alternate embodiment of the closed loop fuel system of the CW PIL of FIG. **1** having a liquid fuel recycling loop.

FIG. **17** is a simplified schematic of an alternate embodiment of the closed loop fuel system of the CW PIL of FIG. **1**.

FIG. **18** is a side elevation of the swing arm of the CW PIL of FIG. **1**.

FIG. **19** is a simplified schematic of an alternative embodiment of the feed inlet of the laser of FIG. **1**.

FIG. **20** is a simplified schematic of an alternate embodiment of the closed loop fuel system of the laser of FIG. **1**.

FIG. **21** is a partial simplified schematic of the laser of FIG. **20**.

FIG. **22** is a simplified schematic of an alternate embodiment of the closed loop fuel system of the laser of FIG. **1**.

FIG. **23** is a partial simplified schematic of the laser of FIG. **22**.

FIG. **24** is a simplified schematic of an alternate embodiment of the closed loop fuel system of the laser of FIG. **1**.

FIG. **25** is a partial simplified schematic of FIG. **24**.

FIG. 26 is a simplified schematic of an alternate embodiment of the closed loop fuel system of the laser of FIG. 1.

FIG. 27 is a partial simplified schematic of FIG. 26.

FIG. 28 is a simplified schematic of an alternate embodiment of the closed loop fuel system of the laser of FIG. 1.

FIG. 29 is a partial simplified schematic of FIG. 28.

DETAILED DESCRIPTION OF THE INVENTION

Turning to the drawings and first referring to FIG. 1, the preferred embodiment of a continuous wave photolytic iodine laser, there shown and generally designated as **10**, comprises a gain cell **12**, an optical system **14** in communication with the gain cell a pair of microwave subsystems **16**, **17**(only **16** is shown), and a closed loop fuel system **18** also in communication with the gain cell.

Below is a list of terms and their definitions as used herein.

I=Intensity

σ^{se}=Stimulated Emissioner Cross Section

ΔX=Distance in cm

RI=Species (RI) concentration

λ=Wavelength

A_{spont}=Einstein Coefficient

g_u=Degeneracy of state "u"

g_{tu}=Degeneracy of state "tu"

Δv=Frequency Bandwidth

V(ω,a)=Voight Profile

Δv_D=Doppler Frequency Bandwith

τ_{spont}=Spontaneous Lifetime

ω=Frequency

c=speed of light

HF=Hydrogen Fluoride

DF=Deuterium Fluoride

COIL=Chemical Oxygen Iodine Laser

Δv_H=Homogeneous Linewidth

F_{UV}=UV Flux

k=Rate Constant

σ_{pump}=Pump Cross Section

I*=different species of Iodine

α_m=small signal gain

P_m=single pass gain length

ϵ=Dielectric Constant

g_1=Degenerate State of 1

I_{Sat}=Saturation Intensity

L=Gain Length

r=reflectivity

R_1=Power Reflectivity

δ=Gas Absorption Loss

δ_C=Total Transmission Loss

T=Power Transmission

N=Concentration of Atoms/cc

F_{IR}=Infrared Flux

CO_2=Carbon Dioxide

CW PIL=Continuous Wave Photolytic Iodine Laser

Process as provided by the present invention are used effectively as models comprised of algorithms executed on computational apparatus of known type to establish laser parameters. In a first process, a kinetics model establishes laser operating parameters such as, pressure, fuel flow rate, and gain cell transverse dimensions. In a second process, a heating ventilation and air conditioning (HVAC) model establishes and optimizes the fuel system's hardware requirements and configuration. The parameters specified when using the kinetics model are flow tubing diameters, numbers and locations of valves, dimensional properties of heat exchangers, condensers and evaporators, and features such as diffusers, plenums, elbows, and transitions to other sizes and shapes. The HVAC model establishes critical design parameters used to create a low friction fuel flow system for the CW PIL of the present invention. The thermal capacity requirements of the ancillary support equipment needed to operate the CW PIL of the present invention are established using results from the kinetics model.

When designing a laser, the dimensions of the transverse gain, the operating pressure, and the fuel flow rate needed to achieve a desired cell output power must be considered. Establishing these parameters provides for the determination of, the mass flow rate of the fuel through the gain region for a given flow velocity. The power output of the laser of the present invention is proportional to the mass flow rate of the fuel through the laser.

The mass flow rate of the fuel determines the required size for the condenser used to convert gaseous fuel exiting the gain cell to a liquid. The mass flow rate of the fuel also determines the size of evaporator, used to convert the liquefied fuel back to a gas, the heat exchangers, and the attendant flow hardware. The size and capacity of the condensers, evaporators, and heat exchangers in turn, determine the size of the low temperature coolers required to control the fuel temperature for the laser fuel system.

A critical parameter in the CW PIL of the present invention is the transverse dimension of the laser gain cell **12**. The gain cell **12** is best seen in FIGS. **2** and **3**. The transverse dimension "t" in FIG. **3** of the laser gain cell **12** is one of the determining factors with regard to defining the microwave pumping subsystem **16** design. Whether the gain cell transverse dimension "t" is 1½, 3, or 6 inches in height effects the shape and structure of the UV lamps **14** and the reflectors **20** used in the laser. Additionally, the transverse dimension "t" governs the number of lamps **14** and their placement. The microwave pumping of the UV plasma lamps of the present invention can best be accomplished at a frequency of 2450 Mhz or 915 MHz. However, the invention should not be limited in this regard as it is also possible to operate at other frequencies.

Based on the foregoing, it can readily be seen that optimization of the design of the laser of the present invention via computer modeling and simulation, prior to building a prototype is provides a cost effective and efficient means for determining the laser's parameters. As such a process is provided by the present invention whereby an integrated PIL model (Kinetics model) based on solving a series of equations using excited iodine (I*) and molecular iodine (I_2), and determining a value for signal gain defines the laser system's configuration. A Rigrod resonator is simulated in the kinetics model to calculate the circulating infrared (1.3μ) intensity in the system. The kinetics model also estimates the outcoupled intensity or power. A finite difference method is used by the kinetics model to solve the series of equations. By using a steady-state approximation for free radical iodine (I) and C_3F_7, denoted hereafter as species (R), the differential equations being modeled were accommodated.

The process employed by the kinetics model provides parameters used in continuous wave (CW) lasers. In addition, the kinetics model of the present invention can study cases of Q-switching, modulation, or other means of varying the laser's duty cycle. This modified kinetics model initially simulates gain pumping without a resonator or circulating infrared flux; once the resonator is simulated, the kinetics model is the same as that for the CW laser with the exception of having accumulated concentrations of I*, I_2, R, and R2.

The kinetics model predicts the behavior of a laser having a gain cell that is 25.4 cm long with a transverse cross sectional area of 1 cm^2. To predict larger transverse dimensions, multiple 1 cm^2 vertical sections can be modeled and simulated. The results are then combined or superimposed, and the behavior of lasers having 1–3 in. high transverse gain cell dimensions was determined. Similarly, additional downstream gain cells can be modeled when the increased input I_2 from an upstream gain cell is added to the kinetics model.

The kinetics model also determines the mass flow rate of the laser's fuel, and the gain cell's **12** pressure. These parameters are then used as the performance criteria for the closed loop fuel system's, item **18** in FIG. **1**, component design. The kinetics model then determines the appropriate hardware configurations for accommodating the calculated mass flow rate of the fuel and the pressure in the gain cell **12**.

The reaction rates whereby the iodine atoms are excited, used in the kinetics model are essentially the same as those used by Schlie and Rathge, as reported in R. D. JOSA, 71(9), 1083 (1981) which is herein incorporated by reference. After reviewing the relevant literature on this subject, these rates seemed representative of nominal values. Many different rates reported in the literature were used in the kinetics model as test cases to explore the sensitivities of the kinetics modeling results to input rates. The following table lists the reactions modeled and the rates used.

Reaction	Acronym	Rate	Units
$RI + h_{v,\,pump} = R + I$	sigmaP	7.80E−19	cm^2
$I^* = I + h_{v,\,rad}$	Arad	7.70E+00	sec^{-1}
$I^* = I + h_{v,\,laser}$	sigmaSE	5.50E−18	cm^2
$I + R = RI$	rate5	4.70E−11	$\frac{cm^3}{sec}$
$I^* + R = RI$	rate6	7.90E−13	$\frac{cm^3}{sec}$
$R + R = R2$	rate7	1.30E−12	$\frac{cm^3}{sec}$
$I^* + RI = I + RI$	rate8	2.80E−16	$\frac{cm^3}{sec}$
$I^* + I + RI = I2 + RI$	rate12	3.80E−31	$\frac{(cm^3)^2}{sec}$
$I^* + I + I_2 = 2I_2$	rate13	3.00E−30	$\frac{(cm^3)^2}{sec}$
$I^* + I_2 = I + I_2$	rate14	9.90E−12	$\frac{cm^3}{sec}$
$I^* + A_r = I + A_r$ + heat	rate15	5.20E−17	$\frac{cm^3}{sec}$

In an effort to closely simulate the actual hardware used, known or estimated efficiencies of hardware components which had been determined experimentally were included in the kinetics model. For example, when 6 kW of microwave energy was input into the kinetics model, the overall efficiency of the laser was calculated as follows:

Efficiencies	Symbol	Values
power supply	ϵ_{pwrsp}	0.9
magnetron	ϵ_{mag}	0.83
UV lamp	ϵ_{uvlamp}	0.45
UV optics	$\epsilon_{uvoptics}$	0.7
quantum efficiency	ϵ_{quant}	0.98
resonator	ϵ_{res}	0.5
UV to IR	ϵ_{uvir}	0.21
resonator/gain area ratio	ϵ_{rgr}	0.9
waveguides	ϵ_{wg}	0.9
Overall Laser	ϵ_{laser}	0.0020

In the CW PIL of the present invention, the microwave subsystems **16**,**17** in FIG. **1** provide power to the UV lamps **14** (see FIG. **3**) such that a laser gain medium is pumped through the gain cell. The ultra violet (UV) pumping power generated by the lamps **14** of the present invention was determined by using the above efficiencies. The UV input to the gain was calculated by:

$$P_{UV} = P_{\substack{wall\\plug}} * \epsilon_{pwrsp} * \epsilon_{mag} * \epsilon_{\substack{uv\\lamp}} * \epsilon_{\substack{uv\\optics}} * \epsilon_{quant} * \epsilon_{uvir} * \epsilon_{wgp} \quad (1)$$

The UV flux was calculated for a 1 cm^2 square, (assuming the UV reflector focused the radiation to a 1 cm wide maximum intensity zone) 25.4 cm long gain cell **12** as shown in FIG. **3** This system required 8.03 kW of input (wallplug) power to give 6 kW of microwave power resulting in 170 W of useful UV power delivered to the fuel. To make this determination, input parameters are entered into the kinetics model as listed below:

INPUT CHARACTERISTICS	VALUE
Microwave Power	6000 watts
Fuel Pressure	20 Torr
Flow (Gain)	100 m/s
Residual Iodine	0 molecules/cm^3
G Width (flow)	1 cm
GL (bulb length)	25 cm
G Height	1 cm
AR (Pressure)	0 Torr

Resonator parameters are similarly entered. Resonators can be of either the "stable" or "unstable" type. Resonators accommodate the characteristics of the active medium and the diffractive properties of the radiation generating in the lasing process. A stable resonator is one that has convergent optics. An unstable resonator has divergent optics. The resonator that was modeled was a stable resonator.

The calculated UV flux to the gain region and the operator selected "starting" IR intensity were:

Fluxes		Value
UV intensity	L_{UV}	3.5613E + 18 photons/cm^2*sec
IR intensity	L_{IR}	4.6396E + 19 photons/cm^2*sec

The UV flux reaching the gain region is denoted as $L_{UV} L_{RI}$, $L_{UV} L_{R2}$, and $L_{UV} L_{R3}$ in 1 cm^2 transverse areas oriented vertically down. The UV flux reaching the gain cells were calculated using Beer's Law.

$$I = I_o e^{-\sigma_{se}(RI)\Delta x} \quad (2)$$

UV Flux Reaching Vertically Oriented 1 cm^2 Transverse Sections (UV source on Top)

Fluxes	Symbol	Layer	Values
Intensity Layer 1	$L_{UV}L_{R1}$	1 cm	3.5613E + 18
Intensity Layer 2	$L_{UV}L_R$	2	8.2853E + 17
Intensity Layer 3	$L_{UV}L_R$	3	2.5701E + 17

As previously stated, to evaluate gain cells of varying heights, 1 cm^2 transverse section are superimposed in layers on one another. For the second and third layers of 1 cm cells (two for the second layer and three for the third), the following equations were used.

$$I=I_o e^{-\sigma_{se}(RI)\Delta x}(0.5) \text{ and } I=I_o e^{-\sigma_{se}(RI)\Delta x}(0.67) \quad (3)$$

The kinetics model is run separately for each 1 cm^2 gain cell, and the results are combined to estimate the total laser performance and behavior for gain sections larger than 1 cm^2. Many other intermediate values are also calculated, such as, concentrations, intensities, etc. These values are displayed on the kinetics model's spreadsheet as the program is run and the calculations proceed. The stimulated emission cross section is given by .

$$\sigma_{se\ modified} = \frac{\lambda_0^2 A_{spont}}{8\pi}\left(\frac{g_u}{g_{tu}}\right) \quad (4)$$

with values tabulated in the literature. The values are fit into a look-up table for the kinetics model spreadsheet using the following relation, with Δv in Mhz.

$$\sigma_{se,\ modified}=400\Delta v^{-0.960} \quad (5)$$

These values include corrections for hyperfine line degeneracies and the Voight profile, V(ω,a).

$$V_{(\omega,a)} = \frac{a}{\pi}\int_{-\infty}^{\infty}\frac{e^{-x^2}}{a^2+(\omega-x)^2}dx \quad (6)$$

where

$$P_{(\omega,a)} = G(\omega) = \frac{1}{\Delta v_D}\left(\frac{\ln 2}{\pi}\right)^{1/2} V_{(\omega,a)} \quad (7)$$

The linewidth, G(ω), is determined by

$$I_{sat} = \frac{4\pi n^2 h v}{\left(\frac{\tau}{t_{spont}}\right)\lambda^2 \eta g(v)} \quad (8)$$

with τ=tspont, η=1, and

$$\frac{1}{g(v)\eta} = \Delta v$$

where Δv is the linewidth.

$$k = \frac{2\pi}{\lambda} = \frac{\omega}{c} \quad (9)$$

The pressure broadened linewidth is determined to be based on the reported 15+/−4 Mhz/Torr for C_3F_7I. The linewidth is calculated for each case on the kinetics model by root-sum-squaring (RSS), both the Doppler linewidth of 400 Mhz (FWHM, at 20 Torr) and the pressure broadened linewidth. Saturation intensity values of 440, 770, and 1150 W/cm^2 are among several reported. Most of these are for COIL lasers, which have kinetics that are considerably different from the PIL kinetics due to the lower pressures, it suggests that I_{sat} may be in the same region. Since hyperfine rates have only been theoretically estimated, firm I_{sat} values have not been established.

$$\Delta v = \sqrt{\Delta v_D^2 + \Delta v_H^2}$$

$$\Delta v = \sqrt{(400)^2 + (1890)^2} = 1890 \text{ Mhz} \quad (20 \text{ Torr})$$

This linewidth is calculated for each pressure used, within the spreadsheet.

The kinetics model addresses the hyperfine levels by assuming a weak collision model. Additionally, it is assumed that any hyperfine level can rapidly relax to any other hyperfine level. Because the velocity and hyperfine cross-relaxation rates are very rapid, the medium is assumed to saturate homogeneously, since all calculations are at pressures of 14 Torr and greater. The small signal gain is treated as being independent of velocity and hyperfine cross-relaxation rates. The temperature dependence of the linewidth is not treated here.

Finite Difference Kinetics Model of Transverse Flow PIL with Rigrod Simplified Resonator using Steady-State Approximation

The rate of change of excited atomic iodine (I*) is described by

$$\left(\frac{dI^*}{dt}\right) = F_{uv}\sigma_{pump}(RI) - k_{I_2}(I^*)(I)(RI) - \sigma_{se}F_{IR}(I^*)(I)(I_2) - kg(I^*)(RI) \quad (10)$$

This steady state approximation makes the kinetics model suitable to run on a PC spreadsheet-based program. It gives reasonably accurate results, and is fast enough, such that sufficient cases can be run to provide trends as parameters are changed and designs varied. A finite difference method is used where (I*) and (I_2) are calculated in time increments assuming that the resonator started with constant CW fuel flow, UV pumping, and stable pressure. Initial concentrations of all species except the fuel C_3F_7I (RI) are zero.

A steady-state approximation is assumed for the gaseous radicals, ground state atomic iodine, and C_3F_7 (R). Due to the rapid rates, the concentrations are assumed to be small and constant. Other species such as I_2, excited atomic iodine (I*), RI, and R2(C_6F_{14}) are assumed to be larger in concentration and variable. The rate of change of ground state atomic (I) is

$$\left(\frac{dI}{dt}\right) = k_1 + (I^*)(I_2) + \sigma_{se}F_{IR}(I^*) + A_{spont}(I^*) - k_5(I)(R) - K_{13}(I^*)(I)(I_2) \quad (11)$$

and the rate of change of radical C_3F_7 (R) is

$$\left(\frac{dR}{dt}\right) = \sigma_{pump}F_{uv}(RI) - k_5(I)(R) - 2k_7(R)^2 \quad (12)$$

This can be simplified to

$$\left(\frac{dR}{dt}\right) = \sigma_{pump}F_{uv}(RI) - k_5(I)(R) \quad (13)$$

To further simplify this model, the three-body deactivation reaction with I_2 is assumed to be slower than the three-body deactivation reaction with the fuel RI . Since the fuel is significantly higher in concentration (40–50 times) than (I_2) levels at all times, the overall rate of excited iodine deactivation is approximately 10 times faster for the fuel three-body deactivation reaction. The spontaneous emission rate is markedly slower than any other rate and is assumed insignificant. Therefore,

$$\left(\frac{dI^*}{dt}\right)= \sigma_{pump}F_{uv}(RI) - k_I + (I^*)(I_2) - \sigma_{se}F_{IR}(I^*) - k_8(I^*)(RI) - k_{12}(I^*)(I)(RI) \tag{14}$$

In order to solve this equation for (I*), the value of (I_2) and the infrared flux, F_{IR}, must be determined, all other values being known. The rate of change of (I_2) is

$$\left(\frac{dI_2}{dt}\right) = k_{12}(I^*)(I)(RI) + \frac{1}{2}\,k_{13}(I^*)(I)(I_2) \tag{15}$$

Again, assuming that the overall rate of excited iodine deactivation is approximately 10 times faster for the fuel three-body deactivation reaction, as described above, this simplifies to

$$\left(\frac{dI_2}{dt}\right) = k_{12}(I^*)(I)(RI) \tag{16}$$

$$\int_{t1}^{t2} dI_2 = \int_{t1}^{t2} k_{12}(I^*)(I)(RI)dt \tag{17}$$

To solve for (I_2), the concentration of ground state atomic iodine (I) must be determined. Using the steady-state approximation,

$$\left(\frac{\partial I}{\partial t}\right) = 0,$$

Equation (12) can be simplified assuming (R2) is small, giving

$$\left(\frac{\partial R}{\partial t}\right) = 0 = \sigma_{pump}F_{uv}(RI) - k_5(I)(R) \tag{18}$$

and

$$\sigma_{pump}F_{uv}(RI)=k_5(I)(R) \tag{19}$$

Solving for (I) gives

$$I = \frac{\sigma_{pump}F_{uv}(RI)}{k_5(R)} \tag{20}$$

Subtracting equation (14) from equation (11) and substituting equation (19) gives the rate of change of excited iodine over incremental time increase (t1 to t2).

$$\frac{dI^*}{dt} = 2\sigma_{pump}F_{uv}(RI) - 2k_1 + (I^*)(I_2) - 2\sigma_{se}F_{IR}(I^*) - k_8(I^*)(RI) \tag{21}$$

$$\int_{t1}^{t2} dI^* = \int_{t1}^{t2} 2\sigma_{pump}F_{uv}(RI)dt - \int_{t1}^{t2} 2k_1 + (I^*)(I_2)dt - \int_{t1}^{t2} 2\sigma_{se}F_{IR}(I^*)dt - \int_{t1}^{t2} k_8(I^*)(RI)dt \tag{22}$$

However, (R) is not known and must be calculated. To solve for (R), a steady state approximation is used where

$$\left(\frac{\partial R}{\partial t}\right) = 0.$$

The rate of change of (R) is

$$\left(\frac{\partial R}{\partial t}\right) = 0 = -\sigma_{pump}F_{uv}(RI) + k_I + (I^*)(I_2) + \sigma_{se}F_{IR}(I^*) - k_{12}(I^*)(I)(RI) \tag{23}$$

Solving for the ground state atomic iodine (I) concentration gives

$$(I) = \frac{\int_{t1}^{t2} (I^*)(k_1 + (I_2)dt + \sigma_{se}F_{IR}dt) - \int_{t1}^{t2} \sigma_{pump}F_{uv}(RI)dt}{\int_{t1}^{t2} k_{12}(I^*)(RI)dt} \tag{24}$$

The concentration of (I_2) can now be determined, and is a sum over the finite difference as a function of time using Equation (16).

$$\int_{t1}^{t2} dI_2 = \int_{t1}^{t2} k_{12}(I^*)(RI)dt \tag{25}$$

The kinetics model is assembled on a spreadsheet, as a finite difference model using

$$\left(\frac{\partial I^*}{\partial t}\right) = -V\left(\frac{\partial I^*}{\partial x}\right) + \frac{\Delta x^2}{2\Delta t}\left(\frac{\partial^2 I^*}{\partial x^2}\right) \tag{26}$$

where V is the linear flow velocity of the fuel. The second term is assumed to be small and Equation (26) becomes,

$$\left(\frac{\partial I^*}{\partial t}\right) = -V\left(\frac{\partial I^*}{\partial x}\right) \tag{27}$$

In traditional flowing gas lasers, the time element

$$\left(\frac{\partial I^*}{\partial t}\right)$$

is transformed into distance downstream

$$\left(\frac{\partial I^*}{\partial x}\right)$$

in the flow as shown in Equation (27), with incident pump energy at the start, or x=0, parameters. However, since the kinetics model of the present invention is assumed to pump uniformly over a significant 1 cm^2 transverse area in the flow direction, the kinetics model is a peculiar mix of finite difference steps in time, with some unknown relation with I* as the gas flows downstream. In other words, the I* versus distance (time increments) curve is similar to, but not actually, the behavior of the I* in the flow direction.

Model Execution

The kinetics model makes several calculations per time (flow distance) increment. The power of the spreadsheet approach is that all intermediate calculations, and all calculated intensities, concentrations, gains, etc. can be displayed easily for each time increment, facilitating better understanding of the kinetics model as well as the laser. The calculation steps taken by the kinetics model are as follows.

Step 1

Calculation of (I*) using equation (22)

$$\int_{t1}^{t2} dI^* = \int_{t1}^{t2} 2\sigma_{pump}F_{uv}(RI)dt - \int_{t1}^{t2} 2k_1 + (I^*)(I_2)dt - \int_{t1}^{t2} 2\sigma_{se}F_{IR}(I^*)dt - \int_{t1}^{t2} k_8(I^*)(RI)dt \quad (22)$$

using values of (I_2), (I^*), and F_{IR} from the previous step.

Step 2

Subtract the (I*) lost to the three-body deactivation reaction.

$$\left(\frac{\partial I^*}{\partial t}\right) = k_{13}(I^*)(I)(I_2) \quad (28)$$

Step 3

Calculate the (I_2) concentration change using Equation (25)

$$\int_{t1}^{t2} dI_2 = \int_{t1}^{t2} k_{12}(I^*)(RI)dt \quad (25)$$

Step 4

Correct the (I_2) concentration for linear fuel flow velocity and the resultant decrease in steady state (I_2) concentration,

$$(I_2)_{corrected} = (I_2) - \frac{I_2(1\text{cm})_{gain\ cell}}{\text{Flow Rate (cm/}s)}\Delta t \quad (29)$$

Note that the (I*) concentration is not corrected for linear flow velocity since the lifetime of excited iodine (I*) relative to the stimulated emission is on the order of one nanosecond at 15–20 Torr, therefore, the flow can thus be considered to be stagnant.

Step 5

Calculate the small signal gain of the laser from the population inversion of the excited state atomic iodine (I*) to the ground state (I).

$$\alpha = \frac{\left(N_2 - \frac{g_u}{g_l}N_1\right)\lambda^2\eta g(\nu)}{8\pi n^2 t_{spont}} \quad (30)$$

where

$$\eta = \frac{\epsilon}{\epsilon_0},\ t_{spont} = \frac{1}{A_{spont}},$$

and

$$\frac{g_u}{g_l} = 0.5$$

Calculate the circulating intensity of the resonator using a simple Rigrod resonator to determine the infrared flux (used in the spreadsheet calculation to calculate the stimulated emission).

$$I_{out} = \frac{I_{sat}}{\left(1 + \frac{r1}{r2}\right)(1 - r1r2)}\left[2\alpha_{mo}L - \ln\frac{1}{r1r2}\right] \quad (31)$$

Where r1 and r2 are the e field reflectivity's of the end mirrors, R1 and R2 are the ϵ^2, or power reflectivities, α_{mo} is the small signal gain, L is the single pass length of the gain, and I_{sat} is the saturation intensity of the laser.

$$R_1 = r_1^2 \quad (32)$$

In delta notation, the transmission and reflectivities of the end mirrors are related by

$$R_1 = 1 - \delta_1 = T_1 \quad (33)$$

$$R_2 = 1 - \delta_2 = T_2 \quad (34)$$

The total loss of the resonator is represented by $\delta_c = \delta_0 + \delta_1 + \delta_2$ where the linear gas sorption loss, do, is assumed to be zero. The losses due to resonator mirrors are

$$\delta_c = \ln\frac{1}{R_i} = 2\ln\frac{1}{r_i} \approx \ln\frac{1}{R_1R_2}\ \text{or,} \quad (35)$$

$$\delta_c = 2\alpha_0 p + \ln\frac{1}{R_1R_2} \approx \ln\frac{1}{R_1R_2} \quad (36)$$

where α_o is assumed very small. The small signal gain in delta notation, δ_m, is presented by

$$\alpha_m = 2\alpha_m p_m \quad (37)$$

where α_m is the gain per cm and pm is the single pass gain length. Also, the loaded gain, α_m, is calculated for homogeneous broadening by

$$\alpha_m = \alpha_{m0} + \frac{1}{1 + \frac{1}{I_{sat}}} \quad (38)$$

Step 7

Return to Step 1 using values determined in this finite Δt (or Δx) incremental step.

Model Details On Starting And Population Levels

On start up of the kinetics model, all concentrations were zero except for the fuel (RI) and all fluxes were zero except for the UV flux, F_{uv}, which is constant. A starting infrared flux, F_{IR}, is used in the second step to initiate the stimulated emission. Due to the mathematical instability of the kinetics model after 40–50 time increments, various techniques were attempted:

a) increasingly fine time increments down to values similar to the rate constants (10–18 s).

b) averaging of ground state atomic iodine (I) values over several time increments steps to dampen oscillations.

c) automatic sampling.

The instabilities were due to the oscillation of concentration of ground state atomic iodine (I). This was determined by fixing the values of each species or parameter in turn or in combination. The kinetics model was relatively insensitive to the circulating infrared flux, F_{IR}, values.

The ground state atomic iodine (I) concentrations were found to oscillate over small levels for several cycles (e.g., between 10–11 and 10–12 molecules/cm^3). Averaging of these values over a series of oscillations and using this average value for the rest of the time steps, eliminated most instabilities in the kinetics model.

Fixing (I) early in the kinetics model's time increments fixes the ground state population, in contrast to clamping of the inversion level for lasing conditions. On the other hand, the complexity of the iodine laser with degeneracies of both ground state and upper states, due to hyperfine levels, makes this approach questionable. The hyperfine levels must be modeled in order to adequately address this problem. The results herein are based on rapid equilibration between both upper and lower states which is generally accepted at higher pressures. As addressed above, the pressure broadened line widths for cases run with this model are large, giving I_{sat} values of 505 W/cm^2 for most cases. Only when very short pulsed operation is modeled would hyperfine levels possibly not contribute. This effect can be described phenomenologically by ascribing an increase in the penetration capability of the higher intensity beams. When the cutting speed for conventional lasers used in manufacturing has been optimized for a particular thickness of material using a conventional laser system, the PIL system of the present invention would be operating in an over-penetration mode. This indicates that the cutting speed when using the CW PIL of the present invention, can be increased significantly.

Pulsing an Nd:YAG FPL does not provide the same power density advantages ecause the cutting rate will be determined by the repetition rate of the laser. A 500 Watt average power laser, operating at 500 Hz, will in the example given in Table II have a normalized feed rate of 40.

The computer models were used extensively during the development of the CW PIL. However, the results of the kinetics model had to be verified for accuracy. Experimental data on CW PILs is very limited. Therefore, since Textron Defense System's (Textron DS) pulsed PIL also uses the fuel C_3F_7I, it was decided that modeling this laser would be a good test case. Since data existed for this laser, it would allow for verification of the CW PIL models. The variables analyzed using the Textron DS PIL included:

1) an orifice plate using pin-fin plate-fin surfaces;
2) two liquid pumps and an iodine scrubber;
3) all tubing, elbows and friction components, as well as, the condenser, and the heat exchangers;
4) gas tubing diameters of 3, 4, 6 and 8 inches and liquid tube diameters of 1 and 2 inches; and
5) pressure of 30 Torr in the gain.

The kinetics models were run by first specifying the temperature, and hence the pressure, of the fuel at the evaporator exit. The desired pressure in the gain region was also specified. Since pressure drops due to friction are velocity dependent, the flow velocity, V, that satisfies all the above specifications is then determined by iteration until the gain cell's pressure is that which was initially specified (or the evaporator temperature can be varied for fixed velocities until the gain cell is at 30 Torr in a steady-state system). The remaining parameter of interest is the mass flow rate of the fuel, a constant for steady state flow.

$$dm/dt=\rho AV \quad (39)$$

The mass flow rate of the Textron PIL was determined within the gain region where all input parameters are specified. The desired temperature and pressure in the gain region were used to specify the density, ρ, within the gain by the ideal gas law. The gain cross sectional area, A, and the fuel's velocity, V, were specified.

The technical results of this study, using Textron DS's PIL, were that

1) using 3 in. piping and approximately 300 Torr in the evaporator results in allowable flow rates in the range of 2–6 m/s, a result comparable to Textron's result with Freon (#134) with a molecular weight similar to C_3F_7I.
2) The fuel flow curve is dominated by the orifice plate.
3) It was also found that, as the tubing diameter is increased, so is the flow rate due to lower frictional losses.

In addition to determining the maximum achievable flow rate through Textron DS's PIL, pressure drops as the fuel moves from the evaporator to the condenser were determined. It was found that:

1) liquid pressure drops are almost independent of the liquid tubing diameter when the diameter exceeds 1 in;.
2) the most noticeable pressure drops are in the liquid stage, yet varying liquid stage hardware sizes, types has minimal effect on the system flow rate and pressure drops. On the other hand, pressure drops in the gas phase were not very noticeable, yet the system flow rate and pressure drops are sensitive to small changes in the gas phase hardware.

The maximum calculated flow rates, using Textron DS's PIL as the model, and for different tubing diameter sizes are shown below.

Tubing Size	Flow
3 in.	6 m/s
4	10
6	18
8	24

Textron DS's PIL uses a "blow down" fuel system whereby an orifice plate is used to govern the character of the fuel flow into the gain cell. Based on the results obtained from running the computer model, it was determined that small holes in the orifice plate do not appear to give supersonic flow as in HF, DF and COIL nozzles. Due to the high molecular weight of the PIL fuel, the equivalent conductance (loss coefficient K) is very high in small holes. Above 1 atm., the laser is not acceptable for commercial purposes due to safety concerns in the case of gas leaks. At a flow velocity in the gain of 20 m/s the pressure in the evaporator is about 2 atm.

To provide for integration in a production setting, the following design capabilities are included in the present invention. The microwave subsystem employs a high voltage power supply (HVPS), integration with the (HVPS) subsystem was accomplished using I/O signals between the PIL's Programmable Logic Controller (PLC) and the power supply's control system. Communications included event and fault status of the laser system and of the HVPS subsystem. The PLC also provided an external fault loop for the microwave subsystem and the HVPS subsystem. The external fault loop addressed adequate supplies of air flow, water cooling, and other support requirements needed for safe operation of the microwave and HVPS subsystems.

The PLC also provides control I/O signals for the (HVPS). These include high voltage on, off, and enable and disable signals. The PLC provides functional control of the HVPS and displays the condition of the microwave and HVPS subsystems either as visual screen displays, printed hard copy outputs, or as digital records. These conditions include HVPS and microwave subsystem voltage, current, fault status, ready and triggered states. Control and display of these systems can also be accommodated by an associated Personal Computer (PC) connected to the PLC.

In addition to the foregoing, system integration of the PIL with commercial machining centers was investigated by contacting several manufacturers. Based on these results, the following design capabilities are included in the present invention to facilitate integration into a commercially available machining center:

1) Digital or analog I/O signals are used to communicate the machine center's event status, voltages, currents, fault status, ready and triggered states.
2) Digital or analog I/O signals establish control between the PLC and the machining center. Conditions of the machining center can be either visual screen displays, printed hard copy outputs, or digital records.
3) Data Highway communication with a PLC is available. Information can be obtained directly from the PLC or

from the PC. Since Data Highway allows interrogation of all the information that is connected to the PLC, then not only is the digital I/O available but also the analog signals. These include pressure and temperature.

The machine center interface of the present invention includes standard digital interfaces, such as RS-232, present on most PCs. Since the PC is connected to the PLC via the Data Highway, then all of the above signals can be obtained and transmitted to the machine center. Also, if the machine center has RS-232 capability then its status can be interrogated.

Because the present invention is intended for use in an industrial setting, several constraining factors had to be considered. Constraints involving output power scaling and UV input power are implemented. Due to the expense of the fuel, its total volume within the closed cycle is minimized in the present design. The entire laser system fits within reasonably sized standard cabinets. The footprint and height of the system has been kept to a minimum so as not to occupy too much shop floor space.

Condenser and evaporator design as well as capacity evaluations were made since heat exchangers and their accompanying cooling/heating systems can dramatically affect the cost of the PIL. As a result, expensive hardware requirements, especially at the condenser, were reduced. Additionally, the system of the present invention does not waste heatants or coolants. As a result, the condenser temperature should be at −38° C. or higher so that lower cost coolers can be used.

System Scaling To Higher Power

Scaling of the CW PIL to higher performance and power, impacts the size and design of the fuel system. Consequently the blow-down method was a means for reducing the required fuel mass flow rates. The blow-down method (use of an orifice plate) combined with a very effective iodine scrubber and low friction fuel delivery system reduces the cooling requirement needs for very expensive ultra-low temperature coolers (operating down to −73° C.). Low cost, high capacity models with cooling down to −38° C. are therefore used. Preliminary modeling results of the CW PIL of the present invention, indicated that maximum flow rates of 10–12 m/s are achievable with a blow-down system, and have highest pressures about 600–650 Torr. These flow rates are similar to those for traditional, well-designed systems. The chief advantage of using the blow-down system is that it eliminates the ultra-low temperature coolers and insulation problems associated with very cold tubing.

Scaling up of the PIL also involves higher UV input power. The kinetics model established the required UV lamp performance and hardware configurations that provide the appropriate boost in laser output power. As the UV pumping power is increased the concentrations of I* and I_2 increase. The increases in the concentrations of these species are approximately linear with increasing UV power.

This determination results in a new gain cell design which takes advantage of the higher flow and UV input power. In order to increase the flow rate through the gain region, required by the higher pressure requirement, and the higher condenser temperature, the gain cell had to be redesigned. The new gain cell design is the result of varying the gain cell dimensions and exercising the HVAC model to determine resultant performance. The result is

1) The gain cell length was doubled from 10 in. to 20 in.
2) The flow diffuser which facilitates the transition from the smaller fuel system conduits to the larger feed inlet conduit was refined.
3) 4 lamps, two on each side of the gain cell, are used.

Different PIL configurations were studied by varying the pressure, orifices, and flow rates. These studies resulted in an optimal design which comprises the following:

1) 45 Torr pressure in the gain region and use of an orifice plate with a conductance K=500.
2) 24 m/s flow rate within the gain region with no need for a blower to enhance flow rate.
3) 6 in. fuel inlet tubing, and 7 in. condenser, evaporator and heat exchangers.
4) A 1 in.×20 in. gain cell having a height of 20 cm. in the flow direction.
5) An evaporator that operates at 0° to 16° C. and a condenser operates at −38° C.
6) A laser output that is 95% of the maximum estimated power.

This design will provide laser output power equivalent to 95% of the maximum estimated power.

Additionally, it was established that if the feed inlet to the gain cell has an interior cross section in the form of a parallelogram, it must include air foils or flow vanes, **116** as shown in FIG. **19**. These foils or vanes **116** provide for a flow which comes very close to being laminar with minimal turbulence. They also insure that the gas flow rate across the paralellogram feed inlet is uniform in all areas.

Alternate Fuels

Two other methods exist for increasing power: 1) use of new UV plasma lamps having more emitted power matched to the absorption lines of the fuel and, 2) the use of alternate fuels which absorb more radiation in the higher output frequencies of existing or new UV lamps.

The fuel flow computer model (HVAC) was extensively used to determine the effect of the use of these higher molecular weight compounds. Alternate fuels C_4F_9I and C, $F_{11}I$, as well as the typical fuel C_3F_7I were evaluated using the HVAC model. The HVAC model did not incorporate a blower and included post-coolers and pre-heaters before the condenser and after the evaporator respectively. Gas phase tubing diameters of 3, 4, and 6 inches and gain pressures of 20, 30, and 45 Torr were modeled. Additionally, 4, 5, and 7 inch heat exchangers, condensers, and evaporators were used with these respective tubing sizes.

The HVAC model starts its calculation at the exit of the evaporator and ends at the liquid stage within the evaporator, $\dot{m}$ having already been determined for the system. For each element described below, changes in pressure and temperature are calculated. These changes are then added to the pressure and temperature input to the element to provide the output data. The HVAC model currently accepts seven types of elements:

1) constant area pipe
2) local effects such as elbows, valves, etc.
3) single phase heaters
4) single phase coolers
5) evaporators
6) condensers
7) simple heat addition of given magnitude, such as heating from the UV lamps.

The two single-phase heat exchangers of the CW PIL of the present invention, use water as the fluid with which heat is exchanged while the evaporator and condenser use polysiloxane due to the extremely low temperatures required by the scrubber for Iodine scrubbing.

Heat is transferred from one fluid to the another through the walls of the tubing in the heat exchangers according to the equation.

$$\dot{Q}=\bar{U}A\Delta T_m$$

with ΔT_m being an average of input and output temperatures. $\bar{U}$ is the mean overall coefficient of heat transfer and depends on the heat transfer coefficients, h, of the two fluids, the thermal conductivity, k, of the tube through which one fluid flows, and the geometry of the tubing in the heat exchanger. "A" is the area available for heat transfer. Note that this equation is hardware dependent through its dependence on $\bar{U}$. Regarding either fluid, the heat transferred can be written as

$$\dot{Q}=\dot{m}c_p(T_{hot}-T_{cold})$$

Geometric input for these heat exchangers consist of

1) the number of pipes in both dimensions,
2) the pipe inner and outer diameter using a built-in table of standard heat exchanger pipes,
3) the pipe spacing in both dimensions and
4) the pipe lengths.

This information is used in the HVAC model primarily to determine the pressure drop across the heat exchanger. The other temperatures and flow rates of the other fluid going through the heat exchanger is also input. Thermodynamic tables for both water and polysiloxane are built into the HVAC model. This provides for determination of the temperature change in the fuel which in turn specifies the required heat capacity of the heat exchanger.

All of the calculations for the heat exchangers (coolers, heaters, condensers, and evaporators) are performed on separate spreadsheets that are linked to the main spread sheet in the HVAC model. This allows great flexibility for using different heat transfer hardware configurations.

Turning now to the condenser, the shell side heat transfer coefficient used in $\bar{U}$ for a condenser is from the standard Nusselt equation for the condensation heat transfer coefficient along banks of horizontal tubes. The saturation pressure is taken to be the entrance pressure. The gaseous fuel coming into the condenser is superheated (i.e. its temperature is well above the saturation temperature determined by the Clausius-Clapyron relationship given above).

This superheat is ignored in the heat transfer calculations so the saturation temperature is taken for the vapor temperature. Since the liquid leaving the condenser is that which has just been condensed, the temperature is also the saturation temperature. The phase change heat transfer (latent) heat of vaporization is hvap. The heat used for just change of state is given by

$$\dot{Q}=\dot{m}h_{vap}$$

the symbol h=enthalpy.

The pressure drop across the condenser is half of that for the input gas going through the same heat exchanger without condensation. An adequate model for pressure drop in two-phase systems is extremely difficult to find in the literature. Apparently, this information is proprietary to the heat exchanger manufacturers. Those pressure drops that are specified are also known to be good to within 50%—a large margin of error.

The evaporator is modeled in the HVAC model as a single (liquid) phase heat exchanger whose output temperature is specified.

The input temperature is that of the liquefied fuel coming out of the condenser. The output temperature was specified during the initial HVAC model setup. By ignoring changes in kinetic and potential energy in the first law of thermodynamics, both reasonably small, it is then assumed that all the heat transferred becomes a change in enthalpy. Since the input and output temperatures are known, the heat transferred is just

$$\dot{Q}=\dot{m}\Delta h$$

Since the fluids are assumed to be ideal, their enthalpies depend only on the temperature. This heat is used in two fashions. The first is during the heat exchange process where again $\dot{Q}=\bar{U}A\Delta T_m$. The other (and typically dominant) heat exchange process is vaporization. The amount of heat going into vaporization was given above by $\dot{Q}=\dot{m}h_{vap}$.

The polysiloxane in the heat exchanger provides the heat for both processes. The pressure drop is taken to be that of a single phase heat exchanger described above since the evaporator is assumed to be flooded. Simple heat addition at a rate of $\dot{Q}$ results in a temperature change of

$$\dot{Q}=\dot{m}c_P(T_{hot}-T_{cold})$$

Major and minor losses and the effect of blowers and pumps are also determined by the HVAC model. These terms are standard in the fluid mechanics discipline and no heat transfer is assumed. Major losses are those that are non-local; i.e. friction losses in pipe flow. The minor losses are local losses; i.e. those due to valves, elbows, bends etc. Major (distributed and frictional) losses are described by

$$h_{loss}=f\left(\frac{L}{D}\right)\frac{V^2}{2g}$$

(head loss)

where L is the length of the pipe considered, D is the hydraulic pipe diameter which is an effective diameter for non-circular cross section pipes, and f is the friction. (Note that here "h" is not enthalpy but head loss, and $\dot{Q}$ is not heat but volume flow rate.) Friction for laminar flow is described by (Reynolds number=Re=VDρ/η<2300)

$f=64/Re$. (Dhydraulic=actual D)

Here V is the flow velocity, D, the hydraulic diameter, ρ the density and η the fluid viscosity.

For turbulent flow (Re>4000), the friction is taken from the Moody chart, which is approximately given by

$$f=\left[1.14-2\log\left(\frac{\epsilon}{D}+\frac{21.25}{Re^{0.9}}\right)\right]^{-2}$$

(ε=the pipe's surface roughness}

The frictional loss is actually flow energy lost to heat; it is a transfer of energy from flow work (the pressure term) to internal energy. The change in internal energy is modeled in terms of a dimensionless irreversible loss coefficient K:

$$K=f(L/D)$$

Minor (local) losses are determined from equivalent conductances, K, which can be found in Tables such as Applied Fluid Dynamics Handbook by R. D. Blevins, ASHRAE Journal, etc. for components such as elbows, valves, orifices, etc.

$$h_{loss}=K\frac{V^2}{2g}$$

A typical equation (incompressible fluid, gas Mach number of <0.3) for a single diameter pipe is

$$\Delta p = \frac{1}{2} K_{total} \frac{\rho V^2}{2} + \gamma \Delta z$$

where K_{total} includes all major and minor losses. When the cross sectional area of the pipe changes, the velocity changes but the volume flow rate $\dot{Q}=VA=\dot{m}/r$ is held constant by conservation of mass.

A pump/blower does work on the fuel to increase its pressure. This can be described by Euler's turbine equation

$$-\frac{dW_{shaft}}{dt} = \rho Q[U_{out}V_{tout} - U_{in}V_{tin}]$$

with u=ωr and V being the tangential component of fluid velocity which is parallel to u. Bernoulli's Equation (first law with no heat transfer) for change in head, H, for a pump efficiency of e_{pump} is

$$\left[\frac{p_2}{\gamma} + \frac{V_2^2}{2g} + Z_2\right] = \frac{e_{pump}}{g}\left[\vec{U}_2 \cdot \vec{V}_2 - \vec{U}_1 \cdot \vec{V}_1\right] + \left[\frac{p_1}{\gamma} + \frac{V_1^2}{2g} + Z_1\right]$$

Conventional PIL systems exhibit large frictional losses. Modeling of both 2 in and 3 in. systems resulted in fuel flow rates of 1–2 m/s in the gain without a pump and 3–5 m/s with a pump, assuming a pressure increase of about 2× times due to the addition of a blower.

The HVAC model results show that a four inch system yielded flow rates of 3–4 m/s without a blower. With a blower, the flow rate increased to 5–6 m/s. Increasing the size of the system to 6 in. diameter tubing and 6 in. valves increases the flow rate to 8–10 m/s without a blower, and to 15–18 m/s with a blower.

The hardware specified in the 4 and 6 in. systems consisted of:

a) straight through gate valves versus angled valves

b) no sharp edged transitions—all edges had ¼ in or larger rolled chamfers.

c) heat exchangers and condensers and evaporators are larger than the overall 4 or 6 in tubing respectively to maintain the low friction design.

d) tubing lengths are minimized

e) elbows are designed with radii large enough to have maximum equivalent conductances

The HVAC model calculates the following parameters:

a) temperature of the fuel.

c) pressure.

d) Reynolds number.

e) gas velocity.

f) delta T and delta P versus pressures reference point in system.

g) kinetic energy of the fuel.

Heating and cooling requirements (external sources) needed in a heat exchanger, condenser or evaporator are also determined by the model.

Due to the high frictional components of the fuel, it is possible to design a system where the pressure drops over the system are too large, and the flow rate cannot be maintained even with perfect condensers and evaporators. The HVAC model indicates this by negative pressures, or negative kinetic energies.

The HVAC model calculates the "manometer" effect of the pressure difference experienced by the fuel liquid phase between the condenser and evaporators. The liquid levels in the condenser and evaporator adjust to the round trip pressure difference by adjusting their heights.

The maximum flow rates were compiled for a variety of cases. The behavior of C_4F_9I and $C_5F_{11}I$ are similar to C_3F_7I. Approximately 30° and 55° C. higher evaporator temperatures are needed for C_4F_9I and $C_5F_{11}I$, than are needed for C_3F_7I which has a higher vapor pressure. Because of the much higher evaporator temperatures, no orifice is needed . Maximum flow rates for these higher molecular weight fuels decreased by about 5–8% compared to C_3F_7I, for the same tubing sizes and gain cell pressure.

Based on the foregoing, it has been determined that the primary driver for lower hardware cost is raising the temperature of the condenser in the present invention from previously typical −60° to −70° C. temperatures to −38° C. This one change significantly reduces the cost of the system by enabling the use of much less expensive coolers.

The most straightforward method of increasing the gain pressure without the use of an expensive pump or blower was to raise the temperature in the evaporator and use the aforementioned blow-down method to reduce the pressure to the right value for optimal laser extraction efficiency.

In addition to determining the maximum achievable flow rate, pressure drops as the fuel moves from the evaporator to the condenser are also of interest. The liquid pressure drops are almost independent of the liquid tubing diameter when the diameter exceeds 1 in. When running the HVAC model, the most noticeable pressure drops are in the liquid stage, yet varying liquid stage hardware sizes and types has minimal effect on the system flow rate and pressure drops. On the other hand, pressure drops in the gas phase are not very noticeable, yet the system flow rate and pressure drops are sensitive to small changes in the gas phase hardware. Dominant pressure drops occur primarily in the gas phase tubing due to tubing lengths, orifice plates, elbows, edges, etc.

A Cu wool molecular iodine scrubber is a necessity in the CW PIL of the present invention since all of the molecular iodine would be carried over from the condenser at the high temperatures of the present invention. As previously stated, the effects of the liquid tubing sections are almost independent of diameter for diameters greater than 1 in.

Important aspects of the hardware design of the present invention are flexibility, modularity, low cost, high performance and simplicity. One type of design modification to the laser to achieve laser output power scaling is to incorporate more UV lamps to pump the gain medium. If the lam,ps are placed such that the gain region is elongated, the flow rate must be increased in order to remove the iodine, a byproduct of the reaction-kinetics that quenches the gain medium, from the longer stretch of active medium. The flow rate must therefore exceed some minimal value. Changes, in the flow rate affect the entire fuel system design.

As already described above, the condenser temperature should be at −38° C. or higher so that lower cost coolers can be used. Specifying the temperature of a saturated fluid specifies the pressure of the fluid. The corresponding pressure is found from the Clausius-Clapyron equation.

$$P_{SAT}=P_{\infty}*\exp(-hfg/RT_{SAT})$$

This equation is plotted in FIG. **4** for the case of the PIL fuel, C_3F_7I. The fuel pressure in the system is also constrained by the optimization of kinetics reactions. Therefore the pressure drop from the gain region to the condenser must be maintained below some specified value. Since both the condenser and evaporator contain both liquid and vapor phases and they are connected by the liquid stage, they form a manometer; the liquid levels adjust to accommodate pressure difference in the associated vapor phases.

The evaporator exit is the only location in the closed loop fuel system in which one can specify the temperature and, by the Clausius-Clapyron equation, the pressure. After the fuel makes a round trip through the closed loop fuel system of the present invention consisting of pressure changes and heat transfer devices, the pressure in the condenser is different from that of the evaporator. According to the first law of thermodynamics, this pressure difference is made up for by a difference in liquid levels in the two heat exchangers **22** and **24** as shown in FIG. **5**. The first Law of thermodynamics for a control volume with multiple inlets and exits in the steady-state is,

$$\frac{dE_{cv}}{dt} = \dot{Q}_{cv} - \dot{W}_{cv} + \sum_{n=\text{input}} \dot{m}_n\left(h_n + \frac{V_n^2}{2} + gZ_n\right) - \sum_{n=\text{exit}} \dot{m}_n\left(h_n + \frac{V_n^2}{2} + gZ_n\right) = 0 \tag{41}$$

with

rate of control volume energy change (0 for steady state)	$\frac{dE_{cv}}{dt}$
average velocity	Vn
mass flow rate (kg/s) (n = a system constant = ρAV)	dmn/dt
gravity	g
height	zn
density	ρ

With no heat addition, work performed, area change or temperature change and with a single inlet and exit, the first law degenerates into the following manometer equation.

$$P_{Exit}+\rho g\ Z_{Exit}=P_{input}+\rho g\ Z_{Input} \tag{42}$$

The CW PIL system of the present invention has intervening heat transfer elements **22** and **24** in FIG. **5**, but still obeys the first law and therefore should still behave as a manometer but with a more complicated first law realization. Therefore, in order to keep both the evaporator **26** and the condenser **28**, operating properly, attention must be paid to the vertical placement of these two devices.

The UV windows **30** and the resonator optics **32** as shown in FIG. **6** must be vertically oriented (perpendicular to the horizontal plane) in order to keep them clean by the action of gravity on any contaminants trying to stick to the windows. This means that the flow must be in the vertical direction as indicated below since only the vertical axis is available. A constraint in the vertical direction is that hardware to get the fuel in and out of the gain region must fit inside the cabinet, which is of limited height.

The hardware configuration within the cabinets must allow for access to all parts that must be reached for repair and/or maintenance. This constraint implies that it is not appropriate to bury subsystems within other subsystems. Laser downtime is expensive to the customer and care must be taken to keep it minimal.

There are several design aspects simplifying the laser of the present invention which reduce hardware needed, and improve performance. These are listed below.

1) Due to short, large 6 in. gas phase tubing and large 1 to 1½ in. liquid phase tubing, no pumps or blowers are required on the fuel system.

2) Heat from exothermic processes is used for heating other parts of the system—the post cooler and preheater are combined into one commercially available crossflow gas phase heat exchanger with tube fin surface.

3) The number of closed loop temperature control, heating and controlled systems is minimized. The heated cooling water from the refrigeration unit used to cool the condenser input into the evaporator to evaporate the liquefied fuel.

The behavior of I* and I_2 as the UV pumping power is increased should also be noted. The increases in the concentrations of these species is approximately linear with increasing UV power. Most of the cases modeled indicated a decreasing improvement in I* (or gain) as the highest UV pump powers were modeled. This may be due to the effects of the increasing concentrations of I_2, at the higher UV pumping levels, decreasing the available gain.

The frictional properties of pipes are usually stated assuming circular cross sections. However, for rectangular cross sections, the "hydraulic" diameter is used in place of the circular diameter. The hydraulic diameter is defined as

$$D_{Hydraulic}=4\ \text{Area}/(\text{Wetted Perimeter})=2*L*W/(L+W)$$

Where L=Length, and W=Width.

for a rectangle. For high aspect ratio rectangular cross sections, as are being considered in the present invention, this formula reduces to essentially,

$$D_{Hydraulic}=2*W+\text{Order}(W/L)$$

Thus, when the gain length is doubled from 10 to 20 in., the hydraulic diameter increases from 1.818 to 1.904 in for a 1 in. width gain and 3.333 to 3.636 in. for the case of a 2 in. width gain. This means that doubling the length has only a minimal hydrodynamic effect. The 20 in. design turned out to require only 20% increased flow versus that of the 10 in. gain cell. Note that for high aspect ratio rectangles, the determination of the loss coefficient, K, is an approximation and the hydraulic diameter is a little smaller than predicted, giving a higher friction. Literature tabulations of

$$k=f*Re$$

were used for 10:1 and 20:1 aspect ratios giving loss coefficients of 84.909 and 89.969, respectively.

Another way in which the fuel flow rate can be increased is to use a shorter gain cell obstruction in the flow direction. The diffusers need not change, just the gain length. All designs of the present invention are for turbulent flow with Reynolds numbers of 5000 or greater. Altering the gain cell design dramatically increases the available fuel flow rate. It also helps the fuel system fit into the vertical constraints of the PIL cabinet. The result of this new design is that the flow rate increases for 30 and 45 Torr systems as shown in the following simulation results.

The first case is the CW PIL of the present invention with a low friction orifice plate (K=500 versus Textron's K=4500), a 45 Torr, long 100 cm gain cell obstruction and a maximum flow rate of 10 m/s with a −38° C. condenser, the results are plotted in FIG. **7**, where curve **74** is fuel pressure in Torr and curve **76** is fuel temperature in 0° C.

The next case is the same system with a 45 Torr, long 20 cm (new) gain cell obstruction and a maximum flow rate with a −38° C. condenser of 24 m/s, shown in FIG. **8**, where curve **78** is fuel pressure in Torr, and curve **80** is fuel temperature in °C. Both 30 and 45 Torr systems were studied. Systems with 20 Torr or lower were not studied because of the larger flow requirements making cooling requirements of the condensers and heat exchangers prohibitive from manufacturing and cost aspects.

For the case of high pressure in the gain cell, using the −38° C. condenser, lower cooling requirements resulted (7–18,000 Btu/hr for 10–24 m/s flow, respectively). See FIGS. **9** and **10**. Referring specifically to FIG. **9**, curve **82** illustrates the evaporator pressure, curve **84** illustrates the pressure before the condenser in torr, and curve **86** illustrates evaporator temperature in °C. for a 100 cm gain cell and an orifice plate having a conductance of 500.

Referring to FIG. **10** curve **88** illustrates the evaporator pressure, curve **90** illustrates the pressure before the condenser in torr, and curve **92** illustrates evaporator temperature in °C. for a 20 cm gain cell and an orifice plate having a conductance of 500.

Comparison between FIGS. **9** and **10** shows that the maximum flow rate increases by approximately 70% (from 14–24 m/s) when the length of the high friction gain cell obstruction is reduced from 100 to 20 cm.

The resulting heat capacity requirement curve, which is essentially the same for both the 100 and 20 cm. gain length is shown in FIG. **11** where curve **94** illustrates the heat capacity in BTU/hr×1000, and curve **96** illustrates the temperature in °C.

For the case of lower 30 Torr pressure in the gain cell, using the −38° C. condenser, excessive cooling requirements resulted (17–28,000 Btu/hr for 10–16 m/s flow, respectively). This is a result of the widening of the UV pumping region to 2 in. (for two opposing UV lamps transverse to the flow) from the 1 inch width at 45 Torr. This doubling of the UV pumping width almost doubles the fuel system mass flow rate for a given flow velocity in the gain.

FIGS. **12** and **13** illustrate the flow rates for given evaporator pressures for systems having a 100 cm long gain cell and the new 20 cm long gain cell, respectively. Referring to FIG. **12**, curve **98** illustrates evaporator pressure, and curve **100** illustrates evaporator temperature. Referring to FIG. **13**, curve **102** illustrates evaporator pressure, curve **104** illustrates evaporator temperature, and curve **106** illustrates the lowest gas pressure in the closed loop fuel system.

Comparison between FIGS. **12** and **13** shows that the maximum flow rate increases by approximately 60% (from 10–16 m/s) when the length of the high friction gain cell obstruction is reduced from 100 to 20 cm. What was expected to make only a marginal increase in flow rate, decreasing the restricted narrow portion of the transverse flow gain area from 100 to 20 cm, resulted in approximately doubling of the flow through the gain. This is with no other changes in hardware, tubing sizes, etc. Accordingly, doubling the flow also doubles the mass flow rate which must be handled by the condenser and evaporator.

The heat removal curves (condenser) and evaporator temperatures for the case at 30 Torr in the gain region are given below in FIGS. **14** and **15** for old (20 cm) and new (100 cm) long gain cells, respectively.

Curve **108** in FIG. **14** illustrates the heat removed by the evaporator, and curve **110** illustrates the evaporator temperature for a 20 cm gain cell. Similarly, curve **112** in FIG. **15** illustrates the heat removed by the evaporator, and curve **114** illustrates the evaporator temperature for a 100 cm gain cell.

Referring again to FIG. **1**, the CW PIL of the present invention is comprised of a gain cell **12**, an optical subsystem **14** communicates with the gain cell, a closed loop fuel system **18**, and a pair of microwave subsystems **16**, **17** (one shown) are also in communication with the gain cell.

Referring to FIG. **2**, the laser's microwave subsystems **16** drive the UV emitting plasma lamps **14**, best seen in FIG. **3**. The lamps **14** are attached to the gain cell **12** such that as they are energized by the microwave subsystems **16**, **17**, the lamps **14** optically pump the laser's gain medium. Referring back to FIG. **2**, the microwave subsystem **16** employs very high powered magnetrons **22** . A single magnetron **22** is capable of driving more than one UV lamp **14**. The means by which this is accomplished will be explained in greater detail below. Using a single magnetron **22** greatly simplifies the microwave systems' **16** electronics, power supply and waveguide requirements. The UV lamps are filled with a gas **13** such as excimer gases or halogen gases which are chosen to match as closely as possible the absorption band of different CW PIL gain mediums, such as, fluoroiodide alkanes, to give greatly increased laser output power and performance. The magnetron **22** is attached to a launcher **24**, and the launcher is attached to a circulator **25**. the circulator **25** is placed in the microwave subsystem to block reflected power and to prevent accidental destruction of the magnetron **22** in the case of a lamp failure. A tuner **28** is attached to the circulator **25** thereby allowing tuning of the microwave resonant cavities **30** and **32**. Wave guide **34** is interposed and coupled to the tuner **28** and tee **31**. Tee **31** is coupled to the resonant cavities **30** and **32**, thereby splitting the microwave power generated by the system to the two lamps **14**, **14** and allowing more than one lamp to be driven by a single magnetron **22**. The tee **31** and waveguide **34** provide the microwave pump radiation to the plurality of UV lamps **14**. The tee **31** in the present invention can be a hybrid (dB reducing) or "magic" tee to insure proper splits of forward traveling microwave power and reduction of reflected or backwards traveling microwave power by routing such power to a water cooled load or other power dump. The lamps **14** on each side of the gain cell **12**, shown in FIG. **3**, are on one focus of a half cylindrical microwave cavity **62** with elliptical cross section, shown in FIG. **2***a*. The cavity **62** communicates with the tee **31**. A microwave-retaining screen **64** is positioned across the cavity **62**. The microwave power generated by the microwave subsystem **18**, is pumped into the UV lamps **14** which subsequently send UV radiation outwardly, substantially perpendicular to the UV lamps **14**. This UV radiation is aimed into the gain cell **12**. During operation, the lamps **14** are cooled in their axial directions via air flowing through the cavity **62**. Adding lamps **14** in the flow direction, supplies additional laser gain to the system. The microwave subsystems **16**, **17** are supported by a swing arm assembly **38**, shown in FIG. **18**, hingedly attached to a support structure **40** such that, the microwave subsystem **16**, **17** can swing away from the rest of the laser, thereby providing greater access to the microwave and lamp assemblies for service and maintenance.

The closed loop fuel system **18** shown in FIGS. **1** and **5** is designed such that maximum power extraction is realized within the laser's gain cell **12** by providing very high gaseous fuel flow rates. The closed loop fuel system **18** is designed for high flow rate/low friction operation. The physical features of the closed loop fuel system were determined using the previously described computer models. The CW PIL of the present invention operates in a regime of higher molecular weight gases, extremes of cold temperatures, and at flow rates far higher than existing systems operate. Thus, the design of the closed loop fuel system is a direct result of exercising the specially built model to handle these very unusual gas flow conditions. Running the kinetics model using optimal hardware dimensions, configurations, and features to optimize the frictional/flow characteristics resulted in several required important features absolutely necessary for very high flow operation.

Additionally, the kinetics model showed that operation at much higher pressures in a CW PIL laser, than previously demonstrated, provides more pumped iodine atoms (for lasing) but, this requires much higher flow rates to push the gain-quenching lasing by-products out of the gain region.

Based on the foregoing, the closed loop fuel system comprises a fuel inlet **42** in communication with the gain cell **12** for receiving and presenting gaseous fuel to the gain cell. The feed inlet **12** of the preferred embodiment consists of a 6 inch diameter tube. By using large diameter tubing, the losses due to the friction of the high molecular weight fuel, namely, C_3F_7I, are minimized. In order to further reduce frictional losses, a diffuser **44** is coupled at its wide end to the feed inlet, and at its narrow end to the fuel delivery conduit **45**, thereby, providing a smooth, low friction transition from the fuel delivery conduit **45** to the feed inlet **42**. It is important that the frictional losses be minimized such that the maximum possible fuel flow rate, without the aid of a blower, can be delivered to the gain cell **12**.

Still referring to FIG. **5**, after the gaseous fuel passes through the gain cell **12**, it enters post cooler **22** where the fuels temperature is lowered prior to entering the condenser **28**. By employing a post cooler **22**, the size and power requirements of the condenser can be reduced. The gaseous fuel flows out of the post cooler **22** and into the condenser **28** where the fuel is converted from a gas to a liquid. As previously explained, the optimal operating temperature of the condenser **28** is −38° C. Operation at this temperature as opposed to the more traditional condenser temperatures of −60° to −70° C. allows for the use of a more economical condenser. Since the gaseous fuel flows from the gain cell **12** immediately into the post-cooler **22**, and the condenser **28** a rapid aerodynamic expansion takes place. This is due to the fact that the gas flows into the condenser **28**, rather than into a tube or channel leading to the condenser **28**. The liquefied fuel passes out of the condenser **28** to scrubber **27**. The purpose of the scrubber **27** is to remove the gain-quenching lasing by-product, I_2. Since I_2 reacts with copper (in one scrubber configuration) to form a precipitate, the scrubber **27** is packed with copper. However, the scrubber **27** is not limited in this regard. The scrubber **27** can be any system **18** which reacts with, precipitates, absorbs, or adsorbs iodine. Since the kinetic rate for this reaction doubles for every ten degrees of temperature increase, the liquid going into the scrubber is heated by heater **33** after exiting the condenser **28** to insure fast and complete reaction with the iodine scrubber materials. After the by-products of the lasing process are removed by the scrubber **27**, the purified liquid fuel is transferred to evaporator **26** where it is converted from a liquid, back to a gas thereby causing a significant increase in pressure which facilitates the transportation of the gaseous fuel through the closed loop fuel system **18**. It was found during the computer modeling and simulations, that the temperature range of the evaporator **26**, should be in the range of 0° to 16° C. Interposed between the condenser **28** and the scrubber **27**, and between the scrubber **27** and the evaporator **26** is the liquid fuel transport conduit **48**. The liquid fuel transport conduit **48** has an inner diameter that is larger than 0.5 in. This was determined by running simulations on the aforementioned computer models. Liquid fuel transport conduits in this size range were determined to be optimal in minimizing friction and thereby pressure losses. In the liquid phase section of the closed loop fuel system, a gear pump **29** is used to increase system pressure to offset any frictional losses. The gear pump's pressure enhancement, when placed in a strategic location, can result in 25–50% increases in the overall system fuel flow rate. Similarly, placement of the system's condenser **28** and post-cooler **22** immediately following the gain cell exit **43** also greatly reduces the frictional gas flow losses, giving increased system gas flow velocities.

After the fuel passes through the evaporator **26**, it is presented to orifice plate **46**. The orifice plate **46** has a series of apertures extending through it as shown in FIG. **5***a*. The orifice plate **46** has a conductivity K=500. While an orifice plate is shown, the invention is not limited in this regard any means such as, a valve, or other obstruction known to those skilled in the art may be substituted without departing from the broader aspects of the invention. The orifice plate **46** is interposed between, and coupled to, the diffuser **44** small end and the conduit **50**. As described in detail above, the closed loop fuel system of the present invention, due to the attention paid to minimizing losses, and the placement of the various components is able to operate at significant fuel flow rates, and pressures, without the need for a blower.

Still referring to FIG. **5**, and in an alternate embodiment, the closed loop fuel system includes a post-cooler **22** interposed between the gain cell **12** and the condenser **28**. The post-cooler reduces the temperature of the spent fuel after it has passed through the gain cell **12**, prior to the fuel's entering the condenser **28**, thereby reducing the power requirements of the condenser **28**. A pre-heater **24** is interposed between the orifice plate **46** and the evaporator **26** for heating the gaseous fuel after it passes out of the evaporator **26** thereby reducing the power requirements of the evaporator **26**. Pressure sensor **52** shown in FIG. **5**, is positioned after the orifice plate **46** with regard to the direction of flow “F”. Pressure sensor **54** is positioned between the post-cooler **22** and the condenser **28**. Pressure sensor **55** is positioned between the evaporator **26** and the pre-heater **24**. Valves **56**, **56** are positioned, with respect to the flow direction “F”, after the post-cooler **22**, and before the pre-heater **24**.

Referring to FIGS. **3** and **6**, because of the high molecular weight gases used for fuel, and the high fuel flow rates, a long rectangular gain cell **12** design carrying multiple lamps **14** along the optical axis **15** can handle approximately the same flow rate as a gain cell with single lamps in the optical axis direction. Thus, twice or higher multiples of lamps **14** can be added to the laser's gain excitation region with minimal loss of gas flow as the gain cell rectangle length increases. The flow model predicts that the determining dimension is “t”, the width of the rectangular gain cell **12**, and not the overall length. Thus, a long gain cell with multiple lamps will support approximately as high a flow rate as a short one. UV lamp windows **58** are mounted flushly to the gain cell **12** such that flow friction is minimized. The UV lamp windows **58** communicate with the gain cell **12** to input UV radiation to the gain cell **12**. Laser windows **60**, for inputting the resonator beam are carried by the gain cell **12**, best seen in FIG. **6**.

In an alternative design multiple UV lamps **14** and microwave cavities can be employed to double the laser gain. Still more pumping power can be achieved by adding more ellipses. The ellipses foci in the gain region must all lie essentially in a horizontal line (coincidental or near-coincidental foci) so the effect of increased pumping is not quenched by laser by-products. At very high flow rates, the kinetics model showed that molecular iodine (I2) concentrations, a by-product of the lasing process which can quench the process if sufficient quantities accumulate, are low enough that two or more microwave pumping regions in the gas flow direction will give almost two more times the gain for two or more times output laser power. Whereas at lower gas flow rates, the kinetics model predicts, and experiments have shown, that iodine concentrations level preclude any lasing downstream of the initial laser gain.

Referring back to FIG. **6** The optical system is comprised of a laser resonator **66** along with beam transfer optics **32**, **32** to shape the laser beam to the appropriate size, and to get the beam out of the CW PIL **10** in FIG. **1**. The resonator **66** is an unstable imaging resonator which provides a flat laser beam phase and intensity at the exit of the laser resonator. This configuration requires a rectangular beam cross section for good transverse mode control.

Referring to FIG. **16**, an optional fuel flow loop **68** is shown. The purpose of the optional liquid fuel flow loop **68** is two-fold. The first is that this loop can be used whenever a gear pump **29** is used as a bypass. The second is that valves **70** can be set so that most of the liquefied fuel can circulate within the loop **68** for multiple passes through the scrubber **27**. Thus the liquefied fuel can pass through the system in a straight through configuration, or using an optional by-pass configuration the amount of exposure time to the iodine scrubber material can be increased.

In another embodiment, shown in FIG. **17**, the post cooler **22** and the pre-heater **24** are replaced by a single cross flow heat exchanger **72**.

In still another embodiment of the present invention, the heater **33**, as well as the condenser **28** and the evaporator **26**, utilize excess heat or coolant from other processes within the CW PIL to cool or heal the laser's fuel. For example, excess heat from the magnetron **22**, shown in FIG. **2** can be used to supply the heater **33** with energy.

In yet another alternate embodiment, the condenser is operated in a "dry sump" configuration. The bottom of the condenser is slanted to a lowest central point with little or no reservoir thereby significantly reducing the amount of fuel needed to operate the CW PIL.

In a still further embodiment of the present invention, the fuel system, gain cell, and resonator designs are applicable to photolytic iodine lasers of less than 100% duty cycle including Q-switched, pulsed, modulated, mode-locked or other modes of non-continuous wave operation.

In a still a further embodiment of the present invention, the fuel system, gain cell, and resonator designs are applicable to photolytic iodine lasers pumped by lamps driven by other sources of pumping power such as continues or pulsed discharge lamps, RF sources. The designs are also applicable to pumping of the PIL gain by direct means such as direct high powered diodes emitting radiation in the PIL's pumping absorbed wavelength.

In yet another embodiment of the present invention, as best seen in FIGS. **20** and **21**, instead of the previously described scrubber, the closed loop fuel system includes a molecular sieve bed **200**, used to remove unwanted iodine (I_2) from the laser's fuel. The molecular sieve bed **200** consists of a hollow vacuum cylinder **202** fabricated from a suitable material, such as, but not limited to stainless steel, and includes vacuum flanges **204** and **206** that are connected respectively to opposed ends of the cylinder. The sieve material **208** is contained within the vacuum cylinder **202** and is composed of a suitable matrix material, such as but not limited to, clay. The molecular sieve bed **200** is positioned between, and in fluid communication with the condenser and evaporator, **28** and **26** respectively. A gear pump **210** is also provided and is in fluid communication with the molecular sieve bed **200** and the condenser **28**. As illustrated in FIG. **20**, the gear pump **210** pumps the fuel from the condenser **26** into the top of the molecular sieve bed **200** where the fuel passes via gravity through the sieve **208** facilitating the removal of the aforementioned unwanted iodine.

Another embodiment of the molecular sieve bed, a pressure fed molecular sieve bed **201** is shown in FIGS. **22** and **23** as being fed from the bottom, however, the invention is not limited in this regard as the molecular sieve bed **201** can be operated in a horizontal or other orientation.

In still another embodiment, shown in FIGS. **24** and **25**, a by-pass loop is provided in connection with either the pressure- or gravity-fed molecular sieve beds, **200** and **201** respectively. In this configuration, a portion of the fuel exiting the molecular sieve bed **200** can be returned for additional passes through the sieve **208** further clarifying the laser's fuel. This is accomplished by adding a return conduit between the molecular sieve bed exit **214** and the pump inlet **216**. A pair of valves **218**, **218** are provided, with one valve being interposed between the molecular sieve bed exit **214** and the pump inlet **216**, and the other valve being located between the molecular sieve bed exit **214** and the evaporator **26**. By throttling the valves **218**, **218** the amount of fuel allowed to recycle back to the pump inlet can be selectively varied, thereby facilitating further iodine removal.

The temperature at which the molecular sieve bed is operated affects its ability to capture the previously described unwanted iodine. As such, and as shown in FIGS. **26** and **27**, a suitable external heat source **220**, such as, heat tapes, band heaters, or coils through which a fluid at the appropriate temperature is circulated, is provided in communication with the vacuum cylinder **202**. Preferably the external heat source is operated to keep the sieve at a temperature between 30°–40 ° F., thereby optimizing its ability to absorb iodine. An additional element important to the proper function of the molecular sieve bed **200** is a pre-heater **222**, positioned between and in fluid communication with the gear pump outlet **224** and the molecular sieve bed inlet **226**.

FIG. **28** illustrates the use of an orifice plate **228** in connection with the above-described molecular sieve beds. The orifice plate is necessary in situations where the concentrations of unwanted iodine in the fuel, as well as the pressure in the closed loop system is low. In operation, the orifice plate **228** causes a restriction in the system which in turn causes the fuel pressure to increase. It is also possible to substitute a valve for the orifice plate.

While preferred embodiments have been shown and described, various modifications and substitutions may be made without departing from the spirit and scope of the present invention. Accordingly, it is to be understood that the present invention has been described by way of example and not by limitation.

We claim:

1. A photolytic iodine laser comprising:

a gain cell, including a resonator having opposed ends and an optical axis said resonator defining an interior cavity; beam transfer optics connected to the opposed ends of the resonator in line with the optical axis; at least one lamp attached to the resonator and in communication with the cavity, a fuel inlet in communication with the cavity for receiving a supply of gaseous fuel, and a fuel exit in communication with the cavity;

a microwave subsystem in communication with the lamp for operating the lamp, such that a gain medium is pumped through the gain cell causing it to lase;

a closed-loop fuel system for presenting the gaseous fuel to the gain cell, including:

- a condenser in communication with the gain cell outlet for converting the gaseous fuel to a liquid;
- a scrubber in communication with the condenser for removing any by-products of the lasing process from the liquefied fuel thereby purifying and preparing the fuel for recycling back to the gain cell;
- pumping means interposed between the scrubber and the condenser for pumping the liquefied fuel;
- an evaporator in communication with the scrubber for receiving and converting the liquid fuel to a gas; and
- said closed loop fuel system pressure causes the gaseous fuel to flow through the gain cell at such a rate as to entrain substantially all of the by-products of the lasing process and transport them out of the gain cell thereby preventing quenching of the lasing process.

2. The continuous wave photolytic iodine laser of claim **1** further including a pressure control means interposed between the evaporator and the fuel inlet member, for controlling the pressure in the closed loop fuel system.

3. The continuous wave photolytic iodine laser of claim **2** wherein the pressure control means is a plate having a plurality of apertures with an equivalent conductance of less than 1000.

4. The continuous wave photolytic iodine laser of claim **2** wherein the pressure control means is a valve.

5. The continuous wave photolytic iodine laser of claim **1** wherein the condenser further includes a coolant inlet for receiving coolant at a minimum temperature of −38° C.

6. The continuous wave photolytic iodine laser of claim **1** wherein the evaporator operates within the temperature range of 0°–16 ° C.

7. The continuous wave photolytic iodine laser of claim **1** further including a heating means interposed between the condenser and the scrubber for heating the liquefied fuel.

8. The photolytic iodine laser of claim **7** wherein the heater comprises a heat exchanger and excess energy generated by the condenser is used to provide heat to the heat exchanger.

9. The continuous wave photolytic iodine laser of claim **1** wherein the feed inlet is a tube having a cross sectional area of at least 7.06 square inches.

10. The continuous wave photolytic Iodine laser of claim **1** further comprising a means for maintaining a pressure of at least 30 torr within the gain cell.

11. The continuous wave photolytic iodine laser of claim **1** wherein the condenser, the scrubber, and the evaporator are connected to each other with tubing having an internal diameter of at least one half inch.

12. The continuous wave photolytic iodine laser of claim **1** wherein the gain cell feed inlet has interior walls and an interior cross section in the form of a parallelogram, a plurality of flow vanes extend from the interior walls to insure both substantially laminar flow of the gaseous fuel and uniform flow across the gain cell inlet.

13. The continuous wave photolytic iodine laser of claim **1** wherein the gain cell is hollow, and rectangular in cross section.

14. The continuous wave photolytic iodine laser of claim **13** wherein the gain cell has a length of at least ten (10) inches.

15. The continuous wave photolytic iodine laser of claim **1** wherein the microwave subsystem includes a magnetron for driving at least two lamps, a launcher in communication with the magnetron, a circulator connected to the launcher for redirection of any back reflected microwave radiation, a tuner for microwave system phase optimization connected to the recirculator, at least one tee connected to the tuners to direct the microwaves along different paths, and waveguides connected to the tees and in communication with the lamps.

16. The continuous wave photolytic iodine laser of claim **15** wherein the at least one microwave subsystem is mounted on a swing arm, the swing arm being mounted by a hinge to a support means so that it can swing away from the laser to provide access to the microwave subsystem.

17. The continuous wave photolytic iodine laser of claim **1** further including a liquid fuel recycling loop comprising at least one valve such that, depending on the valve's position, the liquid fuel can by cycled through the scrubber more than once.

18. The continuous wave photolytic iodine laser of claim **1** wherein the lamp provides radiation in the ultra violet spectrum.

19. The continuous wave photolytic iodine laser of claim **1** wherein the closed loop fuel system further includes a first and second heat exchanger, the first heat exchanger being interposed between the gain cell exit and the condenser for pre-cooling the fuel before it enters the condense, the second heat exchanger means being interposed between the evaporator and the gain cell.

20. The continuous wave photolytic iodine laser of claim **19** wherein the first and second heat exchangers are replaced by one cross flow heat exchanger.

21. The photolytic iodine laser of claim **1** wherein the microwave subsystem is mounted to a swing arm which is hingedly connected to a support surface.

22. The photolytic iodine laser of claim **1** wherein said lamp is driven by an RF source.

23. The photolytic iodine laser of claim **1** wherein the lamps are high powered diodes which emit radiation.

24. The photolytic iodine laser of claim **1** wherein said scrubber removes iodine from the fuel by a respective one of absorption, adsorption, or precipitation.

25. The photolytic iodine laser of claim **1** wherein the microwave subsystem operates at a frequency in the range of approximately 915 to 2450 MHz.

26. The photolytic iodine laser of claim **1** having a control system for regulating said gaseous fuel flow through said closed loop fuel system comprising:

- means for generating concentration signals corresponding to a rate of change in concentration of excited iodine (I*) in the fuel, characterized by,

$$\int_{t1}^{t2} dI^* = \int_{t1}^{t2} 2\sigma_{pump}F_{uv}(RI)dt - \int_{t1}^{t2} 2k_1 + (I^*)(I_2)dt - \int_{t1}^{t2} 2\sigma_{se}F_{IR}(I^*)dt - \int_{t1}^{t2} k_8(I^*)(RI)dt;$$

- means for receiving said concentration signals and generating molecular iodine concentration signals for adjusting a rate at which the concentration of molecular iodine (I_2) in said gaseous fuel changes as the fuel passes through the closed loop fuel system in accordance with a three body deactivation reaction governed by,

$$\left(\frac{\partial I^*}{\partial t} \right) = k_{13}(I^*)(I)(I_2),$$

and

-continued

$$\int_{t1}^{t2} dI_2 = \int_{t1}^{t2} k_{12}(I^*)(RI)dt;$$

means for receiving said molecular iodine concentration signals and generating correction signals to adjust the molecular iodine (I_2) concentration for a linear fuel flow velocity due to a resultant decrease in concentration of steady state (I_2), as characterized by,

$$(I_2)_{corrected} = (I_2) - \frac{I_2(1\text{cm})_{gain\ cell}}{\text{Flow Rate (cm/}s)} \Delta t;$$

means for receiving the correction signals and generating gain signals for controlling the small signal gain of the laser due to a population inversion of the excited state atomic iodine (I^*) to a ground state (I) as evidenced by,

$$\alpha = \frac{\left(N_2 - \frac{g_u}{g_l} N_1\right)\lambda^2 \eta g(v)}{8\pi n^2 t_{spont}},$$

where

$$\eta = \frac{\epsilon}{\epsilon_0},\ t_{spont} = \frac{1}{A_{spont}},$$

and

$$\frac{g_u}{g_l} = 0.5,$$

means for receiving the gain signals and generating intensity signals corresponding to a circulating intensity of the resonator, thereby controlling an infrared flux necessary for regulation of the stimulated emissions from the laser, said intensity signals being characterized by,

$$I_{out} = \frac{I_{sat}}{\left(1 + \frac{r1}{r2}\right)(1 - r1r2)} \left[2\alpha_{mo}L - \ln\frac{1}{r1r2} \right]$$

where r_1 and r_2 are the e field reflectivities, and R_1 and R_2 are the ϵ^2, or power reflectivities, α_{mo} is the small signal gain, L is the single pass length of the gain, and I_{sat} is the saturation intensity of the laser where,

$$R_1 = r_1^2$$

in delta notation, the transmission and reflectivities are related by,

$$R_1 = 1 - \delta_1 = T_1$$

and

$$R_1 = 1 - \delta_2 = T_2$$

the total loss of the resonator is represented by $\delta_c = \delta_0 + \delta_1 + \delta_2$ where the linear gas absorption loss, δ_0, is assumed to be zero;

means for receiving the intensity signals and generating mirror loss correction signals to compensate for losses associated with mirrors in the resonator, as evidenced by,

$$\delta_c = \ln\frac{1}{R_i} = 2\ln\frac{1}{r_i} \approx \ln\frac{1}{R_1R_2} \text{ or,}$$

$$\delta_c = 2\alpha_0 p + \ln\frac{1}{R_1R_2} \approx \ln\frac{1}{R_1R_2} \text{; and}$$

means for receiving the mirror loss signals and generating loaded gain control signals for controlling the loaded gain, α_m, resulting from homogeneous broadening in accordance with,

$$\alpha_m = \alpha_{m0} + \frac{1}{1 + \frac{1}{I_{sat}}},$$

where α_m is the gain per cm and pm is the single pass gain length.

27. The photolytic iodine laser of claim **1** further comprising a heat transfer control system for regulating a rate of heat transfer from and to the gaseous fuel further comprising:

means for generating heat transfer signals corresponding to a rate at which heat is transferred through tubing walls of heat exchangers characterized by,

$$\dot{Q} = \bar{U}A\Delta T_m;$$

means for receiving the heat transfer signals and generating phase change signals determined by sensing the rate at which the fuel passes through and changes phase in the condenser, said phase change being governed by,

$$\dot{Q} = \dot{m}h_{vap};$$

where h=enthalpy,

means for receiving the phase change signals and generating evaporation rate signals to control the rate at which heat is transferred to the fuel as it passes through the evaporator as evidenced by,

$$\dot{Q} = \dot{m}\Delta h;$$

means for receiving the evaporation rate signals and generating major loss compensation signals for adjusting the flow rate of the fuel to compensate for any major losses due to friction in pipes characterized by,

$$h_{loss} = f\left(\frac{L}{D}\right)\frac{V^2}{2g}$$

(head loss)

where the friction f is given by,

$$f = \left[1.14 - 2\log\left(\frac{\epsilon}{D} + \frac{21.25}{Re^{0.9}}\right) \right]^{-2}$$

(ϵ=the pipe's surface roughness};

means for generating minor loss signals that account for any minor losses as evidenced by,

$$h_{loss} = K\frac{V^2}{2g};$$

and

means for receiving and combining the major and minor loss signals to generate pump control signals to control an amount of work done by a pump on the fuel as given by and optimize the pump efficiency as characterized by;

$$-\frac{dW_{shaft}}{dt} = \rho Q[U_{out}V_{tout} - U_{in}V_{tin}];$$

and

$$\left[\frac{p_2}{\gamma} + \frac{V_2^2}{2g} + Z_2\right] = \frac{e_{pump}}{g}\left[\vec{U_2}\cdot\vec{V_2} - \vec{U_1}\cdot\vec{V_1}\right] + \left[\frac{p_1}{\gamma} + \frac{V_1^2}{2g} + Z_1\right]$$

28. A continuous wave photolytic iodine laser comprising:

a rectangular gain cell at least ten inches long for receiving a continuous supply of gaseous fuel, having, an optical axis; beam transfer optics, a laser resonator for shaping a laser beam, at least one lamp positioned along the optical axis, and a fuel inlet and exit;

a microwave subsystem in communication with the gain cell for driving the lamp, such that, a laser gain medium is pumped through the gain cell causing a lasing process to occur;

the microwave subsystem being mounted to a swing arm which is hingedly connected to a support surface; and

a closed-loop fuel system for continuously presenting gaseous fuel to the gain cell, including:

a fuel inlet conduit having, an inner diameter of at least six inches in communication with the gain cell for receiving and presenting gaseous fuel to the gain cell inlet;

a condenser in communication with the fuel cell outlet for converting the gaseous fuel to a liquid;

a scrubber in communication with the condenser for removing any by-products of the lasing process from the liquefied fuel thereby purifying and preparing the fuel for recycling back to the gain cell;

pumping means interposed between the scrubber and the condenser for pressurizing and pumping the liquefied fuel;

a heater interposed between the scrubber and the pumping means for heating the liquefied fuel;

an evaporator in communication with the scrubber for receiving and converting the purified liquid fuel to a gas, thereby causing a further increase in pressure which forces the gaseous fuel through the gain cell;

the condenser, pumping means, heater, scrubber, and evaporator being interconnected by conduit having en inner diameter greater than one half inch;

an orifice plate having a plurality of apertures and a conductance of 500, interposed between the fuel inlet member and the evaporator;

said closed loop fuel system pressure causes the gaseous fuel to flow through the gain cell at such a rate as to entrain substantially all of the by-products of the lasing process and transport them out of the gain cell thereby preventing quenching of the lasing process.

29. A photolytic iodine laser comprising:

a gain cell including a resonator defining an interior cavity and having opposed ends and an optical axis beam transfer optics connected to the opposed ends of the resonator in line with the optical axis; at least one lamp attached to the resonator and in communication with the cavity, a fuel inlet in gaseous communication with the cavity for receiving a supply of gaseous fuel, and a fuel exit in communication with the cavity;

a microwave subsystem in communication with the gain cell for driving the lamp, such that, a laser gain medium is pumped through the gain cell causing a lasing process to occur; and

a closed-loop fuel system for continuously presenting gaseous fuel to the gain cell, including:

a condenser in communication with the fuel exit for converting the gaseous fuel to a liquid;

a molecular sieve bed in communication with the condenser for removing any by-products of the lasing process from the liquefied fuel thereby purifying and preparing the fuel for recycling back to the gain cell;

pumping means interposed between the molecular sieve bed and the condenser for pressurizing and pumping the liquefied fuel; and

an evaporator in communication with the molecular sieve bed for receiving and converting the purified liquid fuel to a gas, thereby causing a further increase in pressure which forces the gaseous fuel through the gain cell.

30. The photolytic iodine laser of claim **29** wherein the molecular sieve bed is gravity-fed.

31. The photolytic iodine laser of claim **29** wherein the molecular sieve bed is pressure-fed.

32. The photolytic iodine laser of claim **29** wherein the molecular sieve bed includes a heating element for selectively maintaining the temperature of the molecular sieve bed.

33. The photolytic iodine laser of claim **32** wherein the heating element is an electrically heated tape wound about an outer periphery of the molecular sieve bed.

34. The photolytic iodine laser of claim **32** wherein the heating element is a coil through which a fluid at a selected temperature is circulated, the coil being wound around an outer periphery of the molecular sieve bed.

35. The photolytic iodine laser of claim **29** further comprising an orifice plate interposed between and in fluid communication with the evaporator and the fuel inlet.

36. The photolytic iodine laser of claim **29** wherein the closed loop fuel system includes a by-pass loop comprising:

a conduit having opposed ends in fluid communication at one end with an inlet to the pumping means, and at an opposite end with the evaporator;

an outlet from the molecular sieve bed being connected to the conduit at a point between said opposed ends of said conduit; and

a pair of valves, one of which is connected to the conduit between the pumping means inlet and the molecular sieve bed outlet, and the other of which is connected to the conduit between the molecular sieve bed outlet and the evaporator.

* * * * *